Journal of South American Earth Sciences 114 (2022) 103687

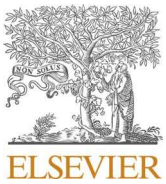

Contents lists available at ScienceDirect

Journal of South American Earth Sciences

journal homepage: www.elsevier.com/locate/jsames

Early and Middle Pleistocene glaciation of the southern Patagonian plain

Corinne Y. Griffing [a,b], John J. Clague [a,*], Rene W. Barendregt [c], Bettina Ercolano [d], Hugo Corbella [e], Jorge Rabassa [f], Nicholas J. Roberts [a,g]

[a] Department of Earth Sciences, Simon Fraser University, 8888 University Drive, Burnaby, BC V5A 1S6, Canada
[b] Department of Earth and Environmental Sciences, Douglas College, 700 Royal Avenue, New Westminster, BC V3M 5Z5, Canada
[c] Department of Geography and Environment, University of Lethbridge, 4401 University Drive, Lethbridge, AB T1K 3M4, Canada
[d] Instituto de Ciencias del Ambiente Sustentabilidad y Recursos Naturales, Universidad Nacional de la Patagonia Austral, Avenida Gobernador Gregores y Piloto "Lero" Rivera, 9400, Río Gallegos, Argentina
[e] Museo Argentino de Ciencias Naturales CONICET, Ávenida Gallardo 490, Buenos Aires, Argentina
[f] CADIC-CONICET, Bernardo Houssay # 200, 9410, Ushuaia, Tierra del Fuego, Argentina
[g] Mineral Resources Tasmania, Department of State Growth, 30 Gordons Hill Road, Rosny Park, Tasmania, PO Box 56, Rosny Park, TAS, 7018 Australia

ARTICLE INFO

Keywords:
Cabo vírgenes glaciation
Great patagonian glaciation
Middle pleistocene
Paleomagnetism
Patagonia
Argentina

ABSTRACT

Evidence of at least three Early to Middle Pleistocene glaciations is recorded in the stratigraphic exposures near the outer limit of glaciation in southern Patagonia. At Cabo Vírgenes, at the mouth of the Strait of Magellan, up to 70 m of till, gravel, sand, and stony silt were deposited in a grounding-line environment at the front of the Magellan lobe along a front several tens of kilometres wide. Accommodation space for the sediments was produced by glacio-isostatic depression resulting from the advance of the Magellan lobe to the Atlantic coast. At that time, the 'moat' in which the sediments accumulated may have been seaward of the modern Atlantic shoreline because the continental shelf is shallow and sea level was much lower than it is today. The sediments at Cabo Vírgenes are normally magnetized, carry no reversed overprints, and thus probably date to the Brunhes Chron (<0.774 Ma). Seacliff exposures south of the Strait of Magellan along the Atlantic coast of northern Tierra de Fuego expose two tills separated by glaciofluvial sediments. Although not dated, the tills record two advances of the Magellan lobe onto the Atlantic continental shelf. The location of the exposures relative to Cabo Vírgenes indicates that the upper of the two tills may correlate with the Cabo Vírgenes drift. The Tres de Enero highway cut, 90 km northwest of Cabo Vírgenes, exposes lodgement tills deposited during the Great Patagonian glaciation (GPG) – two stacked, normally magnetized tills overlie a reversely magnetized till. Truncated sand wedges separate each of the three tills, indicating that the tills record three separate Early to Middle Pleistocene glaciations. The younger of the two normally magnetized tills, and perhaps both, were deposited in the Brunhes Chron; the lowest, reversely magnetized till records extensive glaciation late during the Matuyama Chron (2.608–0.780 Ma). At Bella Vista in the Río Gallegos valley, a 0.89-Ma-old basalt flow caps a thick unit of normally magnetized glaciofluvial gravel, which was probably deposited during the Jaramillo Subchron (1.075–0.991 Ma), but certainly not later. Sediments at Tres de Enero and Bella Vista show that the GPG is not a single event as originally thought, but rather at least three glaciations, perhaps spanning several hundred thousand years.

1. Introduction

Large ice sheets covered much of southernmost South America during Pliocene and Pleistocene glacials (Caldenius, 1932; Mercer et al., 1973; Mercer, 1976; Meglioli, 1992; Bockheim et al., 2009; Coronato and Rabassa, 2011; Rabassa et al., 2011; Coronato et al., 2013). The record of recurrent glaciation, which is among the most complete in the Southern Hemisphere, is well preserved in continental sedimentary deposits and landforms on the southernmost mainland of Argentina and the island of Tierra del Fuego. It provides a valuable proxy of past climate change, particularly for the Early and Middle Pleistocene, a period for which paleoclimate data are sparse in the Southern Hemisphere.

Previous research has shown that Early and Middle Pleistocene ice

* Corresponding author.
E-mail address: jclague@sfu.ca (J.J. Clague).

https://doi.org/10.1016/j.jsames.2021.103687
Received 19 August 2021; Received in revised form 27 November 2021; Accepted 16 December 2021
Available online 20 December 2021

lobes reached the modern Atlantic coast in southern Patagonia (Caldenius, 1932; Meglioli, 1992; Coronato and Rabassa, 2011; Rabassa et al., 2011; Coronato et al., 2013). Well preserved moraines and glaciofluvial landforms record glacier margins related to these extensive advances. However, there has been limited study of the glacial sediments with which the landforms on the Patagonian plain are associated, even though there are excellent exposures along the Atlantic coast and the shorelines of the Strait of Magellan, as well as in road cuts and gravel pits.

A broad chronologic framework for Middle and Early Pleistocene glacials in this region has been provided through radiometric dating of basaltic lava flows that overlie and underlie glacial deposits (e.g. Mercer, 1976; Singer et al., 2004a, 2004b; Griffing, 2018; Clague et al., 2020; Griffing et al., 2020). Most published radiometric ages that constrain the times of these events, however, have been acquired in the eastern foothills of the Andes, far from the sediments and landforms on which the current Patagonian plain chronology is based. Nearer the Atlantic coast, on the western Patagonian plain, are Holocene to late Pliocene lava flows and domes of the Pali Aike Volcanic Field (Fig. 1). Nevertheless, the oldest drift units on the Patagonian plain, which are farthest from the Andes and the subject of this paper, were deposited by glaciers during what has been termed the 'Great Patagonian Glaciation' (GPG) (Mercer, 1976). They lie outside the dated lava flows of the Pali Aike Volcanic Field and thus the number and ages of glaciations and

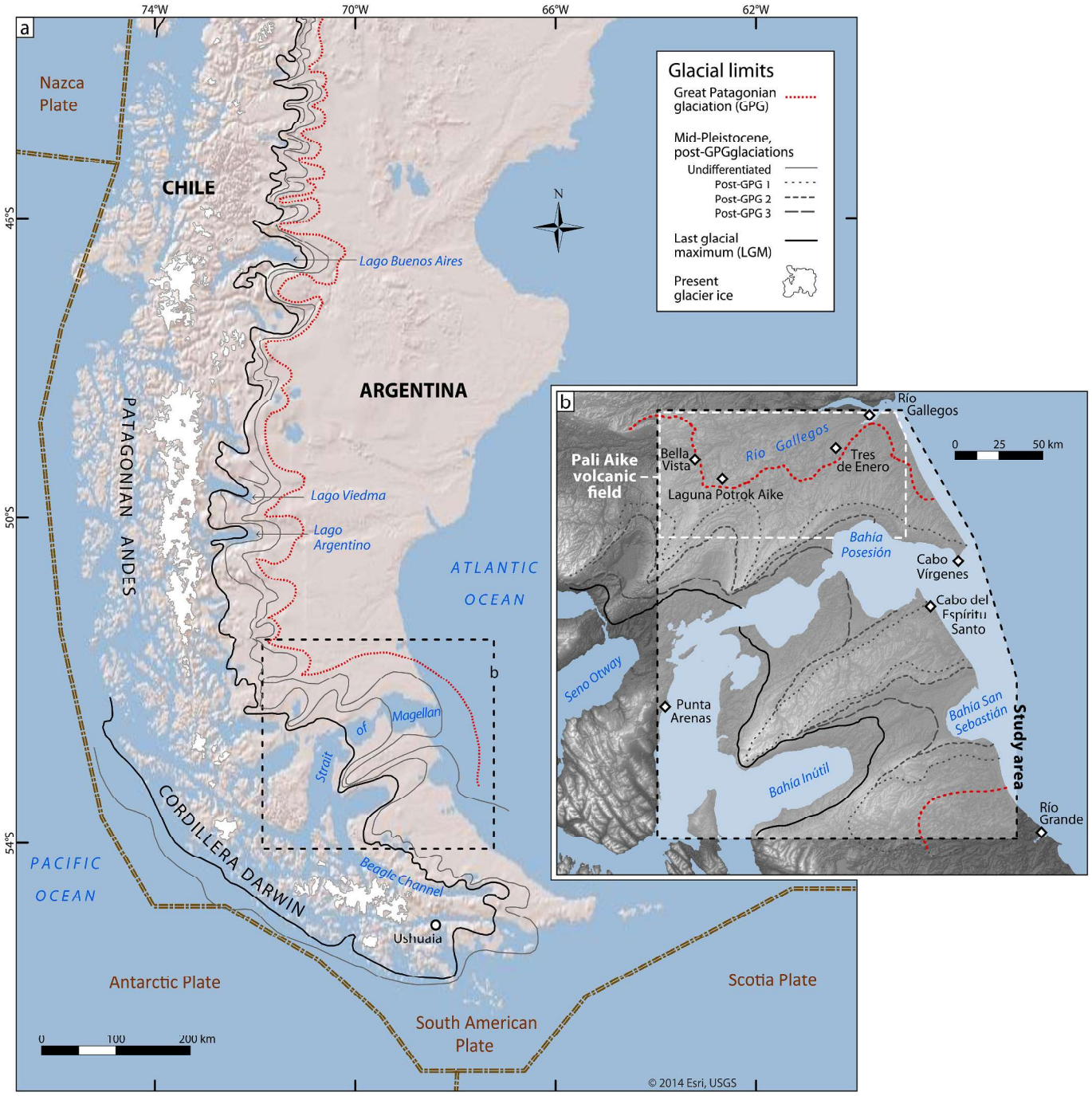

Fig. 1. Map of southern South America showing Pleistocene glacial limits (after Coronato et al., 2004a). Inset DEM shows locations of the field area and Pali Aike volcanic field and is derived from SRTM elevation data at 30-m resolution (USGS EROS Archive - Digital Elevation - Shuttle Radar Topography Mission (SRTM) 1 Arc-Second Global).

their geographic extent on the plains are still not well understood (Rabassa et al., 2011).

Here we present the first regional stratigraphic and paleomagnetic study of Early and Middle Pleistocene continental glacial deposits in southern Patagonia, focusing on the oldest drift units exposed along the Atlantic coast. Our focus is on sediments and landforms assigned to the GPG and a glaciation that followed it, locally referred to as the 'Cabo Vírgenes glaciation'. The use of paleomagnetic techniques allows us to place sequences with confidence in chrons and even subchrons of the Geomagnetic Polarity Time Scale (GPTS), improving the chronology of late Early and Middle Pleistocene glaciations in the region. We correlate the deposits on which the analyses were performed with mapped glacial landforms and discuss the inferred number and ages of glaciations with those recognized by previous researchers.

1.1. Setting

The Strait of Magellan separates the mainland of the continent of South America from Tierra del Fuego and links the Pacific Ocean to the west with the Atlantic Ocean to the east (Fig. 1). To the west are the Patagonian Andes on the mainland and the Cordillera Darwin on Tierra del Fuego, with peaks up to 2500 m a.s.l. These ranges host, respectively, the Southern Patagonian Icefields and the Cordillera Darwin Icefield, which are remnants of the large Andean ice sheet that formed repeatedly over the southern Andean chain during the late Pliocene and Pleistocene. East of the cordillera is the Patagonian plain, which slopes gradually toward the Atlantic Ocean, having been uplifted during the Miocene and incised by rivers and glaciers during the Pliocene and Pleistocene (Rabassa and Clapperton, 1990). The result is an inverted topography, where the oldest surfaces are found at the highest elevations and the youngest surfaces are nested within them at lower elevations (Lagabrielle et al., 2010; Clague et al., 2020; Griffing et al., 2020).

Parts of the southern Patagonian plain are underlain by Upper Cretaceous, Paleogene, and Neogene sedimentary rocks. Notably, the Miocene Santa Cruz Formation comprises mainly nonmarine sandstone and mudstone deposited in the Magallanes Basin between 21 and 14 Ma (Zambrano and Urien, 1970; Ramos, 1989; Perkins et al., 2012, and references therein). The Santa Cruz Formation is unconformably overlain by Neogene basalts (Ton-That et al., 1999; Singer et al., 2004b) and Quaternary sediments, including till, fluvial, glaciofluvial, lacustrine, glaciolacustrine, aeolian, and beach deposits. Quaternary landforms include end, lateral, and ground moraines, drumlins, glacial lineations, meltwater channels, outwash terraces, raised shorelines, and thermal contraction polygons (Mercer et al., 1973; Rabassa and Clapperton, 1990; Meglioli, 1992; Wenzens, 2000, 2006; Rabassa, 2008; Rabassa and Coronato, 2009; Coronato and Rabassa, 2011; Rabassa et al., 2011; Coronato et al., 2004a,2004b, 2013; Clague et al., 2020; Griffing et al., 2020).

The Pali Aike volcanic field, located within the Patagonian plain, comprises basaltic lava flows, scoria cones, and maars that range in age from about 3.3 Ma to the late Holocene (Mejia et al., 2004; Singer et al., 2004b). Volcanism is related to the opening of a slab window in the late Miocene due to subduction of the Antarctic plate beneath the South American plate (Gorring et al., 1997; D'Orazio et al., 2000; Corbella, 2002; Mazzarini and D'Orazio, 2003). Eruptive centres in the Pali Aike volcanic field lie along northeast-trending lineaments and generally decrease in age in that direction (Corbella, 2002).

K–Ar and $^{40}Ar/^{39}Ar$ ages on basalt flows interbedded with tills in the foothills of the Patagonian Andes indicate an initiation of alpine glaciation in the Andes in the late Miocene. The earliest known glacial sediments are about 7 Ma in age; subsequent ice-sheet glaciation occurred during the late Pliocene and Pleistocene (Mercer, 1976, 1983; Mercer and Sutter, 1982; Meglioli, 1992; Ton-That et al., 1999; Wenzens, 2000; Singer et al., 2004a, 2004b; Clague et al., 2020; Griffing et al., 2020).

Researchers have proposed that the Patagonian Ice Sheet first reached the eastern Patagonian plain and the Atlantic continental shelf between about 1.2 and 1 Ma (Mercer, 1976; Meglioli, 1992; Ton-That et al., 1999; Singer et al., 2004b). This early ice sheet extended tens to hundreds of kilometres past late-Pliocene glacial limits, particularly in the Strait of Magellan and along the Bahía Inutil/San Sebastián depression on Tierra del Fuego (Fig. 2). A basalt flow in the Pali Aike volcanic field, which yielded a $^{40}Ar/^{39}Ar$ age of 1.168 ± 0.14 Ma (Singer et al., 2004a), underlies till that includes granitic boulders derived from the Andes. Previous workers consider this age to be a maximum for the time of the most extensive glaciation in this area – the GPG. The best local minimum limiting age for this event comes from the valley of Río Ciake in the Pali Aike volcanic field, where a basalt flow dated to 1.07 ± 0.02 Ma is overlain by drift of the next younger glaciation (Meglioli, 1992).

Meglioli (1992) mapped and correlated drift units north and south of the Strait of Magellan (Fig. 2). He distinguished two coalescent GPG piedmont lobes, one sourced in the Patagonian Andes and the other in the Cordillera Darwin. The GPG surface is characterized by subdued topography with relatively few preserved glacial landforms due to subsequent deflation and fluvial erosion (Meglioli, 1992; Rabassa, 2008). In places, the drift has been so eroded that only erratic boulders remain on the surface. GPG drift is discontinuous between the Strait of Magellan and the Bahía Inútil/San Sebastián depression, occurring as isolated remnants on high surfaces and at its mapped margins (Coronato et al., 2004b).

Post-GPG glaciers were channeled along deep valleys (Fig. 2). The Cabo Vírgenes glaciation, or post-GPG 1 following the terminology of Coronato and Rabassa (2011), is thought to date to between 1.07 ± 0.02 Ma and 0.760 ± 0.007 Ma, based on geomorphic relations and the aforementioned radiometric ages (Meglioli, 1992; Ton-That et al., 1999). Cabo Vírgenes drift consists of till, glaciofluvial gravel, and glaciolacustrine silt and clay (Meglioli, 1992).

2. Methods

We identified, described, and measured sediment units at 107 sites over the course of three field seasons. Stratigraphic sections were chosen based on their relationship to landforms of specific glaciations, accessibility, and the presence of fine-grained sediment suitable for paleomagnetic analysis. We collected most samples from areas previously mapped as GPG and Cabo Vírgenes drift. Stratigraphic units exposed in wave-cut cliffs along the Atlantic coast are continuous over distances of kilometres, whereas inland road cut and gravel pit exposures are typically less than 100 m in length. In the case of coastal exposures, we used the upper limit of tides as a baseline for unit elevations. We measured exposure heights with a laser range finder and recorded sample locations with a handheld GPS. Most exposures, with the exception of those in the Río Gallegos valley and along the Atlantic coast of Tierra del Fuego, had no bedrock at their base.

We used a combination of Landsat ETM+ images (30 m resolution; Global Land Cover Facility, www.landcover.org) and Cnes/SPOT images (2.5–15 m resolution), together with a variety of imagery types from Digital Globe and TerraMetrics to map the glacial geomorphology of the study area at a scale of 1:250,000. We used the surficial mapping protocols established by the Geological Survey of Canada to define landforms (Deblonde et al., 2012), focusing on major moraine ridges, minor transverse ridges (ribbed/Rogen moraines), and marginal scarps and axes of meltwater channels. We considered the glacial limits on the surficial geology maps of Meglioli (1992), Coronato et al. (2004a), and Rabassa and Coronato (2009) in the course of mapping.

We described sediments using standard lithofacies codes (Eyles et al., 1983; Evans and Benn, 2004). Observations include unit thicknesses and elevations, particle size and sorting, color, depositional and deformation structures, presence or absence of fossils, and the nature of unit contacts. At some sites, we measured the trend and plunge of 50 rod-shaped pebbles in near-vertical, cleaned exposures of till with a Brunton compass. Only stones with an a-axis more than two times longer than the

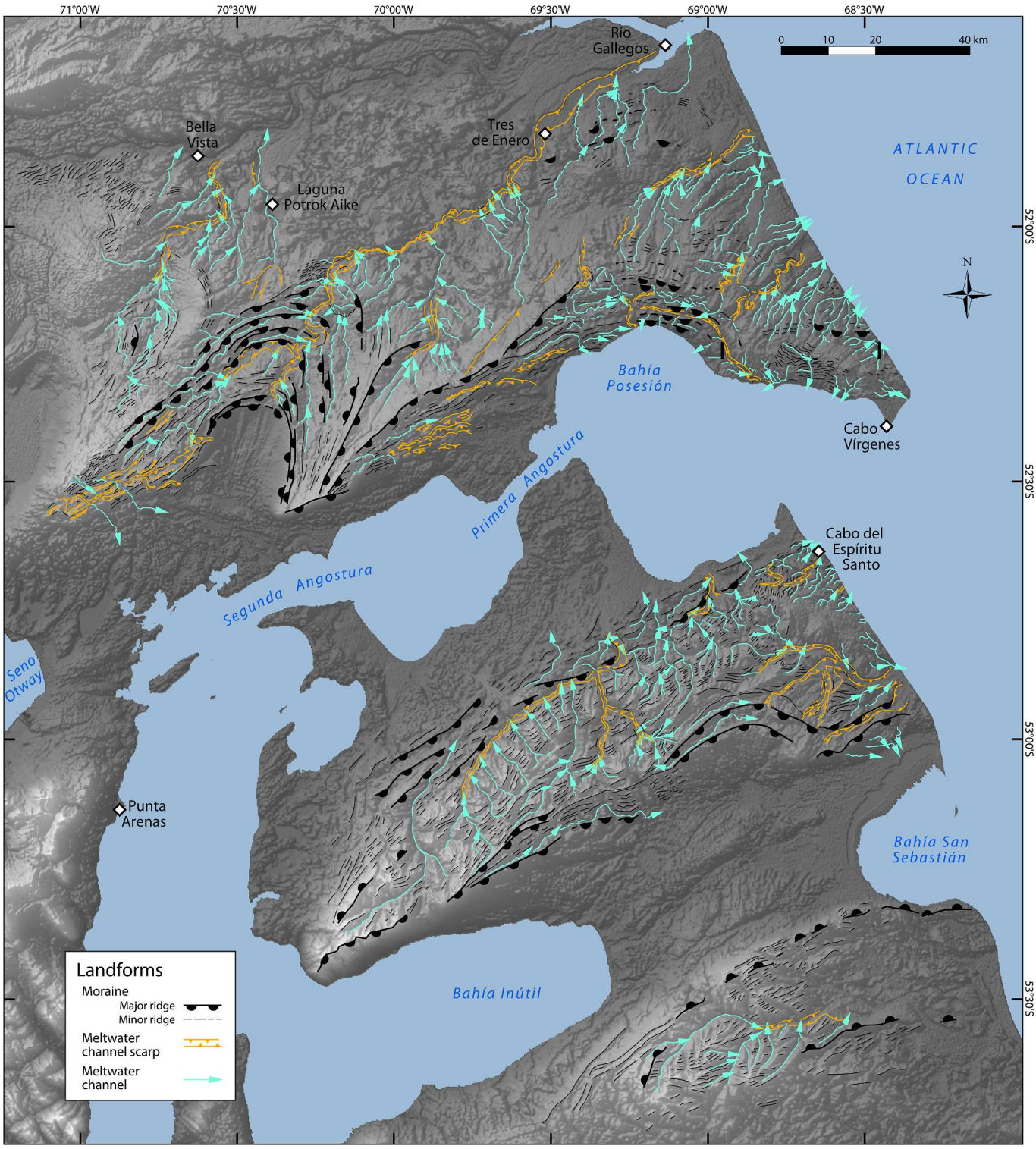

Fig. 2. Moraine ridges and meltwater channels in the study area (modified from Griffing (2018). DEM derived from SRTM elevation data at 30-m resolution.

b-axis were measured. We plotted the orientations of the stones on the lower hemisphere of a stereonet (Schmidt equal-area projection) to infer glacier flow directions (see Griffing, 2018 for additional details).

We collected 642 samples from sediment units that ranged from clayey silt to fine sand for paleomagnetic analysis. Fine-grained sediment was chosen for measurement of remanent magnetism because small ferromagnetic grains are the strongest recorders of past magnetic fields (Butler, 1992). Alignment of coarser ferromagnetic grains is commonly influenced by depositional processes; thus sediment coarser than fine sand was not sampled. Weathered sediments and sediments containing pebbles also were avoided. Most samples were collected from lenses of silt and very fine to fine sand within till and glaciofluvial gravel. Samples were collected by driving polycarbonate plastic cylinders (2 cm diameter x 2 cm length) horizontally into cleaned, vertical, in-situ sediment exposures. Where possible, a minimum of six oriented samples were collected from each layer or lens.

Magnetic measurements were made in the paleomagnetic laboratory at the University of Lethbridge, Alberta. We measured magnetic susceptibility with a Sapphire Instruments (SI–2B) susceptibility meter. We measured the magnetization of each sample with an AGICO JR-6A spinner magnetometer prior to demagnetization and again after each level of stepwise AF demagnetization in peak fields up to 180 mT using an ASC Scientific D-2000 demagnetizer with a three-axis manual tumbler.

The sediments have a high and stable magnetization with paleofield directions within the range of the geocentric axial dipole for these sampling latitudes and are therefore good recorders of the magnetic field. We determined directions of characteristic remanent magnetization for each sample by principal component analysis (Kirschvink, 1980) using Remasoft version 3.0 (Chadima and Hrouda, 2006). Mean characteristic remanent magnetization directions were calculated for each site and an overall mean was also calculated. In a few cases, we used the intersection of great circles to obtain mean directions. Only mean directions with α_{95} values $\leq 25^{\circ}$ were used (in almost all cases α_{95} values were $\leq 15^{\circ}$). The inclination mean for each sample group was compared to the time-averaged geocentric axial dipole direction (GAD) for the study area (52°).

3. Results

We first summarize the geomorphology of the study area and then describe sediments exposed in the key sections on which this paper is based. These sections are a subset of a larger body of data assembled and reported by Griffing (2018) in her unpublished PhD thesis. Paleomagnetic results are summarized in a third subsection.

3.1. Geomorphology

The landscape of the study area has been shaped by Early and Middle Pleistocene glaciation. During major glaciations, an ice sheet formed over the southern Andes and extended eastward to, and in some instances beyond, the present Atlantic coast. Researchers have previously documented a series of successively less extensive advances based on well preserved glacial landforms (Figs. 1 and 2; Meglioli, 1992; Coronato et al., 2004a, 2004b, 2013; Coronato and Rabassa, 2011; Rabassa et al., 2011).

Meltwater channels and moraine ridges dominate the landscape in the area (Fig. 2). We differentiated several generations of meltwater channel systems by tracing them back to the moraine ridges where they initiate and also from channel cross-cutting relations. Meltwater channels are of two general types. Proglacial channels extend in a more-or-less perpendicular direction away from ice margins, typically moraine ridges. Most are wide and flat-bottomed, particularly in the proximal zone. Lateral meltwater channels are located along the margins of moraines. They are common on higher elevation, gently sloping GPG surfaces at the margins of the Strait of Magellan and the valley sides of the Bahía Inutil/San Sebastián depression.

Moraine ridges are linear to arcuate in plan view. They are morphologically diverse, ranging from wide and flat to relatively narrow with sharp crests. Heights range from a few metres to tens of metres. Many moraines in the eastern part of the study area, nearer the Atlantic coast, form discontinuous arcs and broad subdued, but still hummocky, ridges that mark limits of older glaciations. These moraines have been lowered and subdued by aeolian processes. Minor moraine ridges are common on the proximal side of major moraine ridges, ranging from smaller recessional ridges similar in morphology to major end moraines to smaller discontinuous transverse ridges resembling ribbed or de Geer moraines.

3.2. Stratigraphy

We recorded detailed stratigraphic and sedimentologic descriptions at 107 sites, and cursory observations at 30 other localities. This paper focuses on five key sites (Cabo Vírgenes, Cabo del Espíritu Santo, Tres de Enero, Chimen Aike, and Bella Vista; Fig. 1). The Cabo Vírgenes site, located at the Atlantic entrance to the Strait of Magellan, was chosen because of its continuous 36-km-long seacliff exposure spanning the boundary between the GPG and Cabo Vírgenes drift sheets as mapped by Meglioli (1992). The Cabo del Espíritu Santo site, at the Argentina-Chile boundary on northeastern Tierra del Fuego, provides excellent seacliff exposures of GPG and post-GPG 1 drift as mapped by Meglioli (1992). The Tres de Enero site provides an exposure of three stacked GPG tills and cryogenic features, and was chosen because it is representative of sediments observed at other smaller sections in the area. What are possibly the oldest glacial sediments found in this study are till and glaciolacustrine sediments exposed in a small borrow pit near Estancia Chimen Aike, 12 km southwest of Río Gallegos. A road cut along Ruta 40 near Estancia Bella Vista exposes thick outwash gravel underlying a basalt flow of the Pali Aike volcanic field. We include this section in the paper because of the constraint the dated flow provides on Middle Pleistocene glaciation in the area.

3.3. Cabo Vírgenes

The seacliffs north of Cabo Vírgenes provide continuous exposures of Pleistocene sediments deposited during two Pleistocene glaciations (Figs. 3 and 4). Meglioli (1992) mapped the surface as mostly GPG (his 'Sierra de los Frailes drift'), with end moraines of the Cabo Vírgenes glaciation to the west nearer the lighthouse at the mouth of the Strait of Magellan (site TDF113 in Fig. 4). Steep, rapidly eroded coastal bluffs reach a maximum height of 70 m in the vicinity of the Cabo Virgenes end moraine and decrease in height northward with increasing distance from the inferred Cabo Vírgenes ice front. The contact with underlying bedrock is not exposed.

We made observations at 45 sites along the 30-km length of the exposure (Figs. 4 and 5). Stratigraphic columns for the 45 sites are presented in Appendix Fig. 1. Fig. 6 shows our interpretation of the stratigraphy of the exposed sediments at the type section of the Cabo Virgenes drift at the Cabo Vírgenes lighthouse, and Figs. 7 and 8 are photos of typical lithofacies and sedimentary structures of the units exposed in the seacliff. The exposed sediment package is divisible into three stratigraphic units. The upper two units (CV1 and CV2) can be traced over nearly the entire length of the transect, whereas a lower unit (CV3) is exposed discontinuously at the base of the cliffs along the northern half of the transect (Figs. 5 and 7).

The uppermost unit (CV1) comprises interlensing, tan-colored, matrix-supported diamicton, sand, and gravel. Rip-up clasts, ramping, and soft-sediment deformation structures, including flame and ball-and-pillow structures, are present within the unit along the length of the exposure (Fig. 8). The lower contact of the unit is locally erosional, but elsewhere conformable and in a few places loaded (Fig. 8c). Diamicton dominates unit CV1 at some sites, especially along the southern part of transect near the lighthouse. It is massive to weakly stratified and has up to 25% polylithic clasts up to boulder size. Facets and striations are visible on many clasts, clearly indicating a glacial genesis. Rip-ups of underlying gravel or sand up to tens of metres across are common within unit CV1; they are sufficiently cohesive to retain their original stratification, although many are warped or folded (Fig. 8b).The diamicton matrix is silty fine to medium sand. Bedded sand and gravel, ranging from thin (<0.25 m) lenses (Figs. 6 and 7a, b) to bodies more than 5 m thick and tens of metres in length are present within diamicton of CV1 (Fig. 8c). Some, but not all lenses are deformed (Fig. 8d). Sand lenses comprise massive to planar bedded, well sorted, fine to coarse sand, locally with bands of pebbles; some of these lenses infill erosive channels with eroded basal contacts. Gravel lenses are composed of sub-angular to rounded, polylithic, pebble-to boulder-sized clasts and are moderately to well sorted, with a fine to very coarse sand matrix. Planar horizontal bedding is dominant, although cross-beds were also

Fig. 3. Quaternary sediments exposed continuously over a distance of 36 km in the seacliff north of Cabo Vírgenes (photo by Hugo Corbella). The locations of field sites along the seacliff are shown in Fig. 4.

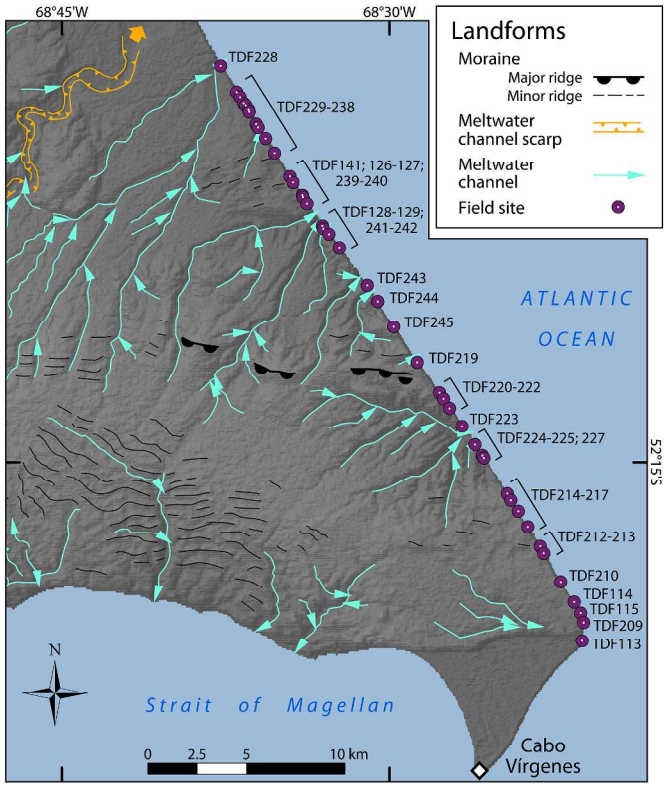

Fig. 4. Field sites and glacial landforms along the Atlantic coast at and north of Cabo Vírgenes.

observed. Some channel fills have a layer of coarser clasts or rip-ups of underlying sediment at their base. The lower contact of unit CV1 loads and deforms unit CV2 in some exposures along the north half of the transect (Fig. 8c). The coarse nature of unit CV1 has resulted in differential erosion of the cliff face by the sea. The upper part of the cliff face, where unit CV1 crops out, is slightly recessive relative to the lower part, which is dominated by unit CV2 (Fig. 3).

Unit CV2 is a weakly stratified to massive, light grey diamicton with a poorly sorted matrix of clayey silt and very fine to fine sand (Figs. 6–8). The diamicton contains about 15% clasts ranging from pebble to cobble size; some of the clasts are striated and faceted. Lenses of massive silt and sand and beds of gravel are present, but are much less common than in unit CV1. Many of these lenses and beds are undeformed, although some display ductile or brittle deformation. The sand and silt lenses are up to 5 m in length, whereas some gravel beds are tens of metres long and up to 4 m thick with erosive lower contacts and little or no deformation. The base of unit CV2 is below beach level along the southern half of the transect, but the contact with unit CV3 is locally exposed to the north, where it is erosional and locally delineated by a thin sand or gravel bed (Fig. 7f). A bulk sample of the diamicton matrix from unit CV2 contained no marine shells, diatoms, or foraminifera (Janice Brahney, personal communication, 2016).

Unit CV3 crops out along the northern part of the seacliff, within 2 m of beach level (Fig. 7e and f). It is a massive, dense, tan-colored diamicton with a sand/silt matrix and 20–25% polylithic pebbles and cobbles, many with facets and striations. This unit differs from unit CV2 in being much more highly consolidated and in having a coarser matrix and higher stone content. The contact between the two units is planar and nearly horizontal; CV3 was not affected by the soft-sediment deformation that shaped units CV1 and CV2, and thus is assumed to be the product of an earlier glaciation. The base of unit CV3 is not exposed anywhere along the Cabo Vírgenes transect.

Units CV1, CV2, and CV3 are incised by broad meltwater channels that terminate at the Atlantic shoreline (Fig. 2). The channels are graded to positions 1–2 m above present sea level (Fig. 5) and are floored by up to 5 m of oxidized planar-to cross-bedded gravel. The surface gravel directly below the floors of the channels is cryoturbated with steeply inclined clasts, and is cut by sand wedges (Griffing, 2018).

3.3.1. *Cabo del Espíritu Santo*

The Cabo del Espíritu Santo seacliff faces the Atlantic Ocean at the northeast corner of Tierra del Fuego at the Argentina-Chile boundary, 31 km south of Cabo Vírgenes. The geology at this location differs from

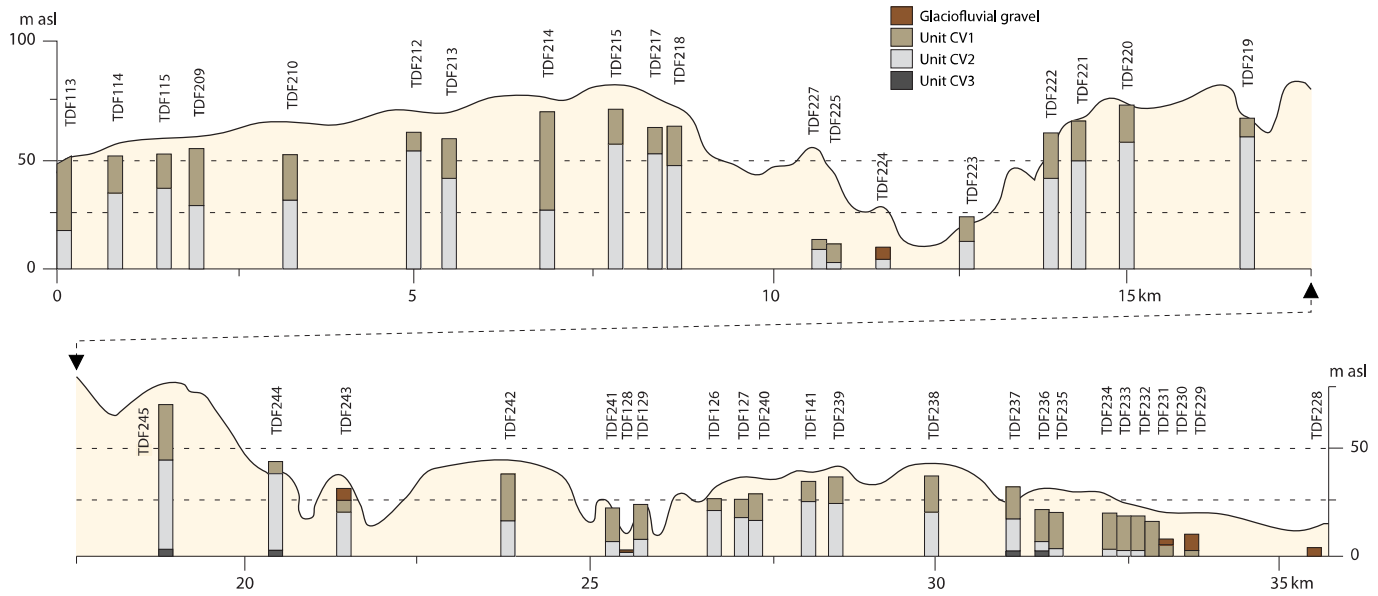

Fig. 5. Simplified geology of sections along the Cabo Vírgenes transect (see Fig. 4 for site locations). Glaciofluvial gravel associated with meltwater channels is incised into units CV1, CV2, and CV3.

that north of the Strait of Magellan in that bedrock crops out up to tens of metres above sea level in most exposures.

The section shown in Fig. 9 is representative of the stratigraphy observed in the 2.5-km-long transect that we documented. The cliff is capped by 0.8 m of massive, dark brown sand with scattered pebbles and cobbles at the base (unit ES1). The sand overlies 2.2 m of massive, matrix-supported, olive-grey diamicton with 5–10% clasts up to cobble size, many of which are striated and faceted (unit ES2). Sand wedges penetrate the upper 0.8–1 m of this unit (Fig. 9a, d). Unit ES2 unconformably overlies up to 4.7 m of well sorted, grey-brown sand and gravel with cross-beds that indicate flow to the southeast (unit ES3). The unit is reversely graded, with fine sand at the base and gravel at the top. It has a sharp, undulating, erosional lower contact. In places, the lower contact of unit ES2 extends down to the top of unit ES4; presumably unit ES3 has been removed in these places by erosion prior to deposition of unit ES2. The sand-gravel unit unconformably overlies 2.5 m of olive-grey matrix-supported diamicton with 25% clasts that are up to cobble size (unit ES4). The upper part of the diamicton is massive, whereas the lower part is weakly stratified. Many clasts within the diamicton are striated and faceted. The lower contact is sharp, undulatory, and erosional. A glacially striated pavement at the base of the diamicton indicates ice flow toward the southeast (150°) (Fig. 9f). This direction aligns with the ice-flow direction of 150–330° inferred from the clast fabric of ES4, which although weak is unimodal. Unit ES5 comprises up to 3.6 m of trough cross-bedded sand with some pebbles and cobbles. The cross-beds indicate flow to the southeast, and S-folds that deform the base of the unit indicate overriding stresses in the same direction (Fig. 9e). Upward, the unit coarsens and becomes more poorly sorted and more weakly stratified. Unit ES5 has an erosional contact with underlying Upper Cretaceous mudstone. Laterally, this unit is missing, presumably having been eroded by the glacier that deposited unit ES4.

The seacliff exposures at Cabo del Espíritu Santo are incised by large meltwater channels that are part of a large glaciofluvial drainage system associated with a post-GPG glaciation (Fig. 2; Meglioli, 1992; Coronato et al., 2004b). The valleys of this channel system are up to 1 km wide, flat-floored, and partially filled with sediment after incision. The modern streams in the valleys are underfit and meandering.

3.3.2. *Tres de Enero*

The Tres de Enero exposure is a ~270-m-long highway cut in GPG drift, as mapped by Meglioli (1992). The height of the exposure ranges from 2 to 6 m. Three till units with stone lags along their contacts are exposed at the site (Fig. 10). The uppermost diamicton (unit TE1) is matrix-supported, massive to weakly stratified, and contains 15–20% pebble- and cobble-size clasts, many of which are striated and faceted. The matrix consists mainly of silt and sand. Some lenses of coarse sand and gravel up to 30 cm long are present within unit TE1. Sand wedges composed of massive to vertically laminated, medium to coarse sand extend downward from the top of unit TE1 (and are spaced about 1–3 m along the exposure (Bockheim et al., 2009). Satellite imagery shows a possible well developed thermal-contraction network on the ground surface at and around the Tres de Enero site, with fractures of similar spacing to those in section. A soil up to several tens of centimetres thick with columnar peds and a dark brown color is developed on unit TE1 (Fig. 10f). The clast fabric measured in unit TE1 is weak, with a mode at about 80–260° (Fig. 10b), which is similar to the north-to-northeast ice flow direction expected for the GPG ice lobe based on geomorphology. Unit TE1 overlies unit TE2 across a sharp erosional contact marked by a discontinuous stone line.

Unit TE2 is a massive, tan-colored, matrix-supported diamicton with 10–15% clasts up to boulder size and a silt-sand matrix. Many clasts are striated and faceted. Sand wedges extend down from the top of the unit; they are more widely spaced than those in unit TE1 and are truncated at the contact with that unit. The contact between units TE2 and TE3 is sharp and marked by a weak stone line and change in color. A weak polymodal to girdle-shaped clast fabric has a mode at about 150–330° (Fig. 10b). Unit TE3 is a massive to weakly stratified, tan-colored diamicton, similar to unit TE2. It is identified as a separate unit because at least one sand wedge within the upper part of unit TE3 is truncated at its contact with unit TE2 (Fig. 10d). In addition, the darker color and columnar structure of the top of the unit may record a sub-aerially weathered surface. Lenses of gravel and sand are common in this unit. Discontinuous stone lines within unit TE3 suggest exposure and reworking of the drift surface and may indicate more than one glaciation or, alternatively, an oscillating ice front during a single glaciation. A weak polymodal to girdle-shaped clast fabric measured at the base of the unit has a mode at 150–330° (Fig. 10b).

A channel filled with gravel and sand cuts through all three diamicton units at the south end of the road cut (Fig. 10e). The channel fill is overlain by matrix-supported, weakly stratified diamicton and is penetrated by sand wedges that appear to be the same generation as those in unit TE1.

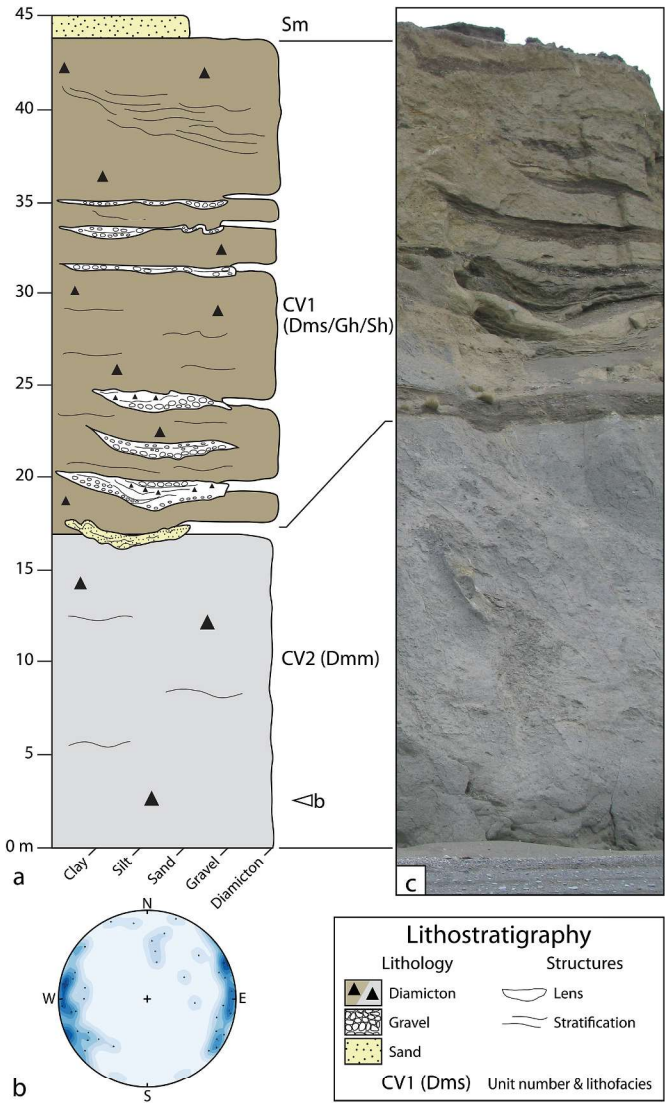

Fig. 6. Type section of Cabo Vírgenes drift (TDF113 in Fig. 4). a) Interpreted stratigraphy. Sm = massive sand; Dmm = massive diamicton. Dms = stratified diamicton; Gh = horizontally bedded gravel; Sh = horizontally bedded sand. b) Contoured stereonet showing orientation of rod-shaped stones at the base of unit CV2 (lower hemisphere projection). c) Photograph of the exposure.

3.3.3. *Estancia Chimen Aike*

What are possibly the oldest sediments found in this study are exposed in a small borrow pit approximately 12 km southwest of Río Gallegos (Fig. 11). About 3.2 m of bedded and laminated silt and sand overlie poorly sorted sandy gravel in the pit walls. The silt/sand sequence comprises (from top to bottom): 0.7 m of massive fine sand with load structures at the base; 1.75 m of rippled, very fine sand to fine sand; and 0.75 m of planar-laminated silt that grades downward into rippled, very fine sand and silt. The sediments are gently inclined and lack visible fossils. Because they are about 10 m higher than the wide Río Gallegos floodplain just to the north, the silt and sand were likely deposited in an ice-proximal lake or pond. Till, which presumably underlies the gravel near the base of the borrow pit, is poorly exposed about 200 m to the northeast along Ruta 40.

3.3.4. *Bella Vista*

A ~30-m-high road cut on the south side of Ruta 40 near Estancia Bella Vista exposes a 20-m-thick sequence of horizontally bedded outwash gravel with minor sand interbeds overlying sandstone and mudstone of the Miocene Santa Cruz Formation (Fig. 12). The gravel contains rounded to sub-rounded clasts, mostly pebbles, but with some cobbles and small boulders. Cross-bedding within the unit indicates down-valley deposition by the paleo-Río Gallegos. The gravel is capped by 6 m of basalt that yielded $^{39}Ar/^{40}Ar$ ages of 0.857 ± 0.032 Ma (Mejia et al., 2004) and 0.89 ± 0.03 Ma (Corbella et al., 2014). In view of the thickness of the gravel and its vertical distance above the modern floodplain of the Río Gallegos (ca. 12–32 m), we interpret it to be outwash deposited during a period of aggradation driven by an advance of a glacier to the west.

3.4. *Sediment paleomagnetism*

The magnetic susceptibility of sediment samples ranges from 120 to 4800 × 10^{-6} SI/vol and averages 850 × 10^{-6} SI/vol. Most samples display magnetizations characteristic of magnetite and have a relatively high magnetic stability for glacial sediments.

Magnetic polarities can be confidently assigned to most of the sampled units (Fig. 13). Appendix Table 1 presents Fisher-averaged directions of each unit and their assigned polarities. Fig. 14 shows examples of well behaved, normal- and reverse-polarity demagnetization data. Stereographic plots of unit means and their 95% confidence intervals, grouped by polarity, are shown for the GPG and Cabo Vírgenes drifts (Fig. 15, Table 1).

The mean remanent magnetization direction of all samples has a declination of 6.5° and inclination of −66.5° (n = 642, k = 2.8, α_{95} = 4.2; Appendix Table 1). A few sites have mean inclinations that are shallower than the expected GAD inclination of 68.6°, and some have larger cones of confidence (α_{95}) about the mean direction, which may be due to the coarseness of the sampled units or the lower quality acquisition of detrital remanent magnetization during deposition. Compaction or deformation of sediments can also result in a shallowing of the inclination of magnetization (Butler, 1992).

Normal magnetization was recorded at nearly all sample sites, including Cabo Vírgenes and Cabo del Espíritu Santo (Fig. 13). Reversed magnetizations are recorded at only four of the 89 sites sampled. These four sites include Estancia Chimen Aike and Bella Vista (Fig. 13). All of the reversed samples are from sites beyond the Cabo Vírgenes drift limit and within the GPG limit. The reversely magnetized sites (nine units at four sites; Appendix Table 1) have a mean inclination of 41.6°, mean declination of 166.6°, α_{95} of 19.4, and a k of 8.0. The relatively large circle of confidence and lower precision parameter reflect the much smaller number of reversely magnetized samples. The shallower inclination of the reversely magnetized samples may, in some cases, indicate incomplete removal of overprints, compaction and/or dewatering of sediment, or the presence of coarser multi-domain grains. The combined GPG samples (irrespective of sign) have a mean inclination of −73.5°, which is slightly steeper than, but still in reasonable agreement with, the GAD for the region (Table 1; Fig. 15).

4. Discussion

4.1. *Cabo Vírgenes*

The sediments exposed along the Cabo Vírgenes transect can be linked to landforms to the west. A west-trending moraine intersects the Atlantic coast ~20 km north of the cape (Fig. 16, location 1). Although subdued, it can be traced as an arcuate area of higher elevations (ca. 80 m a.s.l.) at the coast (Fig. 16, location 3) parallel to the Strait of Magellan and about ~10 km north of the location of the Cabo Vírgenes limit mapped by Meglioli (1992). Ice-marginal and ice-proximal sediments were deposited north of the moraine; their approximate northern limit is delineated by the line that intersects the coast at location 2 in Fig. 16. Proglacial meltwater channels extend in a north-northeast direction away from the moraine and incise units CV1, CV2, and CV3 (e.g. Fig. 16, location 3). The channels presumably formed when ice retreated

Fig. 7. Characteristics of and relations among units CV1, CV2, and CV3 in the Cabo Virgenes seacliff. a) Units CV1 and CV2 at section TDF113. The contact between the two units is locally sharp and erosive, but is commonly gradational and loaded. b) Gravel lenses tens of metres long within diamicton of unit CV1 near section TDF221. c) and d) Stony silty clay (Unit CV2). e) Units CV1, CV2, and CV3 at section TDF245. f) Sharp erosional contact between units CV2 and CV3 at section TDF244.

south-southwest into the Strait of Magellan at the end of the Cabo Vírgenes glaciation.

Numerous small, parallel, slightly sinuous, closely spaced ridges inboard of the end moraine (Fig. 16, location 4) presumably are aligned perpendicular to the direction of glacier flow. The ridges may be subglacial landforms that record grounding of the Strait of Magellan lobe in a body of standing water. The lack of foraminifera and marine shells in the Cabo Vírgenes sediments suggest that this water was fresh, not marine. At one site in this area, the surface is underlain by metres of highly folded and faulted stratified diamicton, sand, and silt (Fig. 17). Clastic dikes cut through these glaciotectonized sediments, indicating pressurized dewatering, perhaps due to stresses exerted by overriding glacier ice. Dewatering of unit CV1 is further indicated by soft-sediment deformation of many diamicton, gravel, and sand interbeds along the coastal transect.

We hypothesize that the retreating glacier either stabilized when it reached location 5 (Fig. 16, white dotted line) or that the moraines at location 6, just west of location 5, were constructed during a younger (Punta Delgada) glaciation, as proposed by Meglioli (1992). Large lateral meltwater channels (Fig. 16, location 7) are present along the margins of this belt of moraines.

The presence of conformable and loaded contacts between units CV1 and CV2 indicates uninterrupted and probably rapid deposition of up to 70 m of sediment during the Cabo Vírgenes glaciation. We infer that subglacial and proglacial meltwater streams carried large amounts of sediment from the Patagonian Andes to the Atlantic coast during this glacial. The thick glacial deposits, which are continuous for 36 km, require large accommodation space in the terminal area of an ice lobe. Further, the characteristics of the drift sheet at Cabo Vírgenes, summarized below, suggest that they were deposited in standing water, rather than on land.

Interfingering of stratified diamicton with poorly sorted sand and gravel (unit CV1) and large-scale loading of unit CV2 by unit CV1 indicate deposition in standing water and delivery of sediment to the area by sediment gravity flows. We hypothesize that this happened on a subaqueous morainal bank comprising a series of fans located close to or

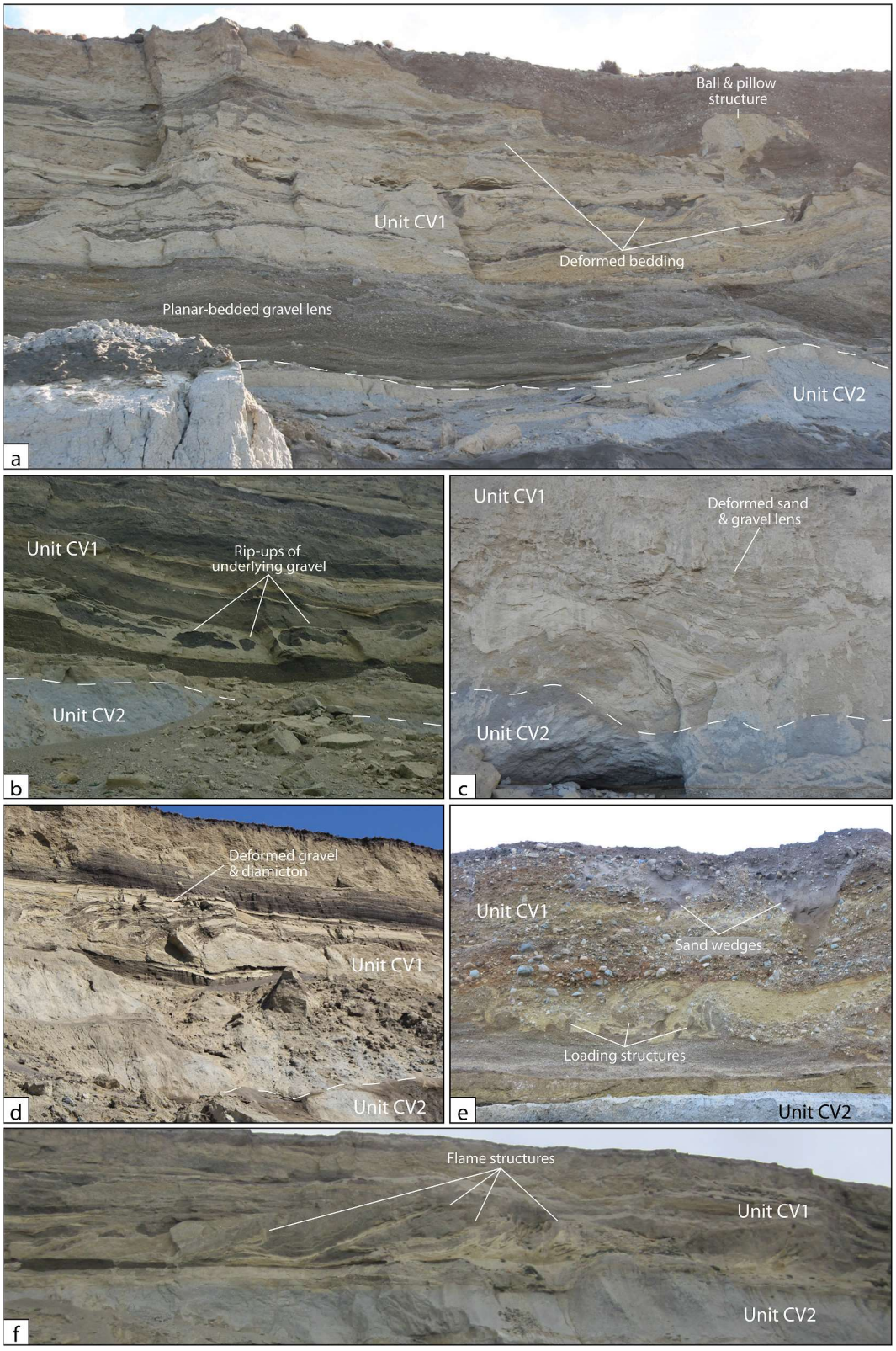

Fig. 8. Deformation structures in sediments exposed in the Cabo Virgenes seacliff. a), d) and e) Deformed bedding in interlensing gravel and diamicton in unit CV1, sections TDF209, TDF214, and TDF224, respectively. Note sand wedges in e). b) Gravel rip-ups near the base of unit CV1, TDF115. c) Deformed lenses of sand and gravel within diamicton at TDF235. f) Flame structures in unit CV1.

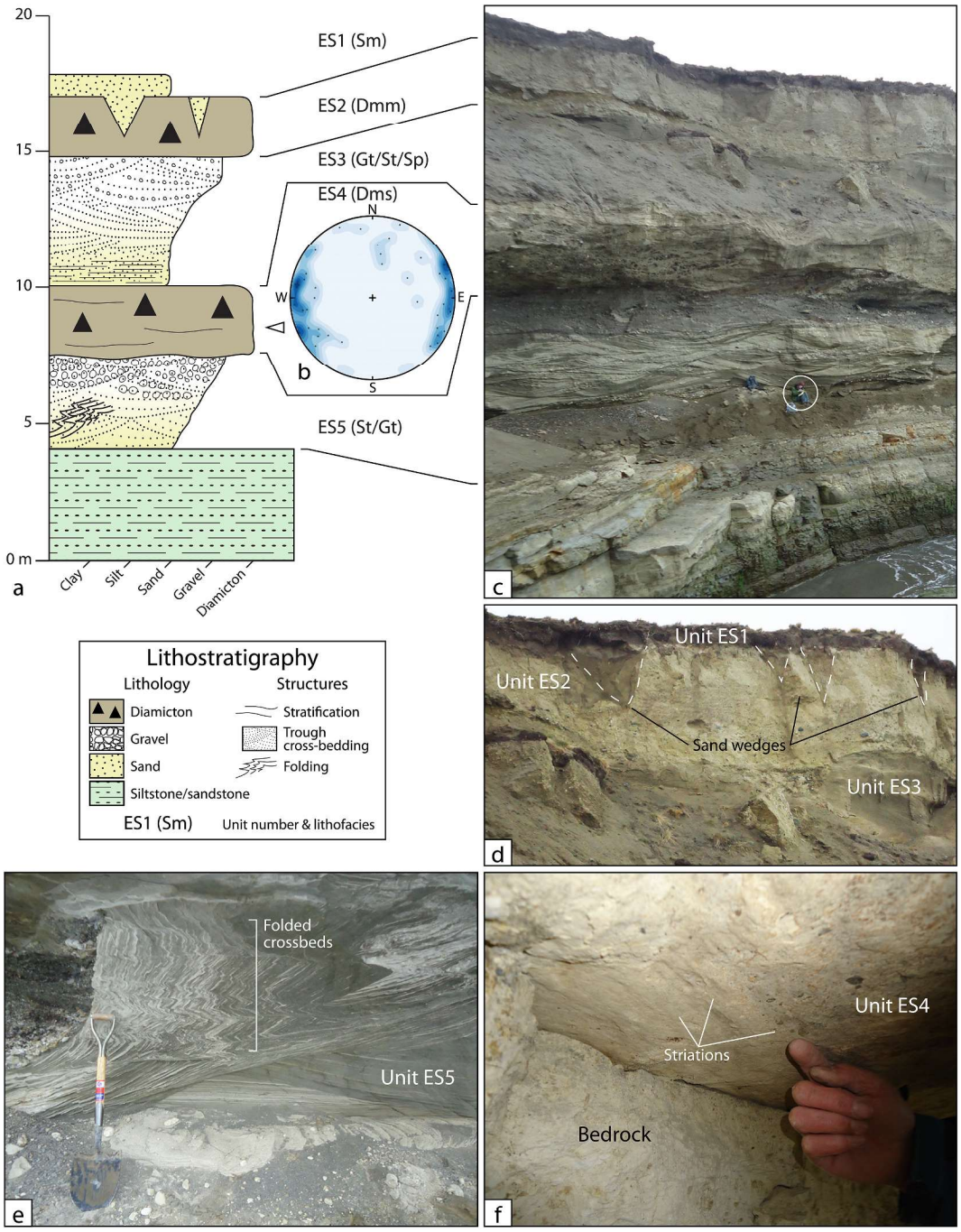

Fig. 9. The Cabo del Espíritu Santo section. a) Stratigraphic column. b) Contoured stereonet showing long-axis orientation of rod-shaped stones at the base of unit ES4 (lower hemisphere projection). c) Photo of the exposure; circled person for scale. d) Sand wedges within unit ES2. e) S-folds at the base of unit ES5. f) Striations along the lower contact of unit ES4 where it lies directly on bedrock.

at a grounding line (e.g. Powell and Alley, 1997; Bennett et al., 2002; Powell and Cooper, 2014) (Fig. 18). A grounding-line environment best explains the lateral variation in unit thicknesses, lithologies, and the pronounced penecontemporaneous deformation of units CV1 and CV2. Sand and gravel sequences within unit CV1 may record deposition at the exit points of tunnels carrying strong meltwater flows. Interfingering of diamicton, sand, and gravel is consistent with ice-marginal subaqueous glacial deposits, as meltwater streams and fan apexes commonly change location due to changes in the subglacial drainage system and the ice margin (Bennett et al., 2002). Development of subaqueous grounding-line moraines and fans is influenced by bathymetry. Deposition along the Cabo Vírgenes ice margin must have occurred in shallow water, where calving rates are relatively low and fans could build up quickly over a short period of time. In contrast, deep-water environments have high calving rates, which encourage rapid ice retreat and do not favor development of extensive subaqueous moraines.

Processes involved in constructing grounding-line morainal banks include: slumping of supraglacial debris into standing water; release of englacial and subglacial debris below the water line during iceberg calving; deposition of sand and gravel from water flowing out of subglacial tunnels; and deposition of diamicton that is carried to the grounding line from the subglacial deforming layer and, in some cases, deformed by ice-push (Boulton, 1986; Powell, 1990; Benn and Evans, 2010). Tunnel mouths may migrate rapidly and frequently along the

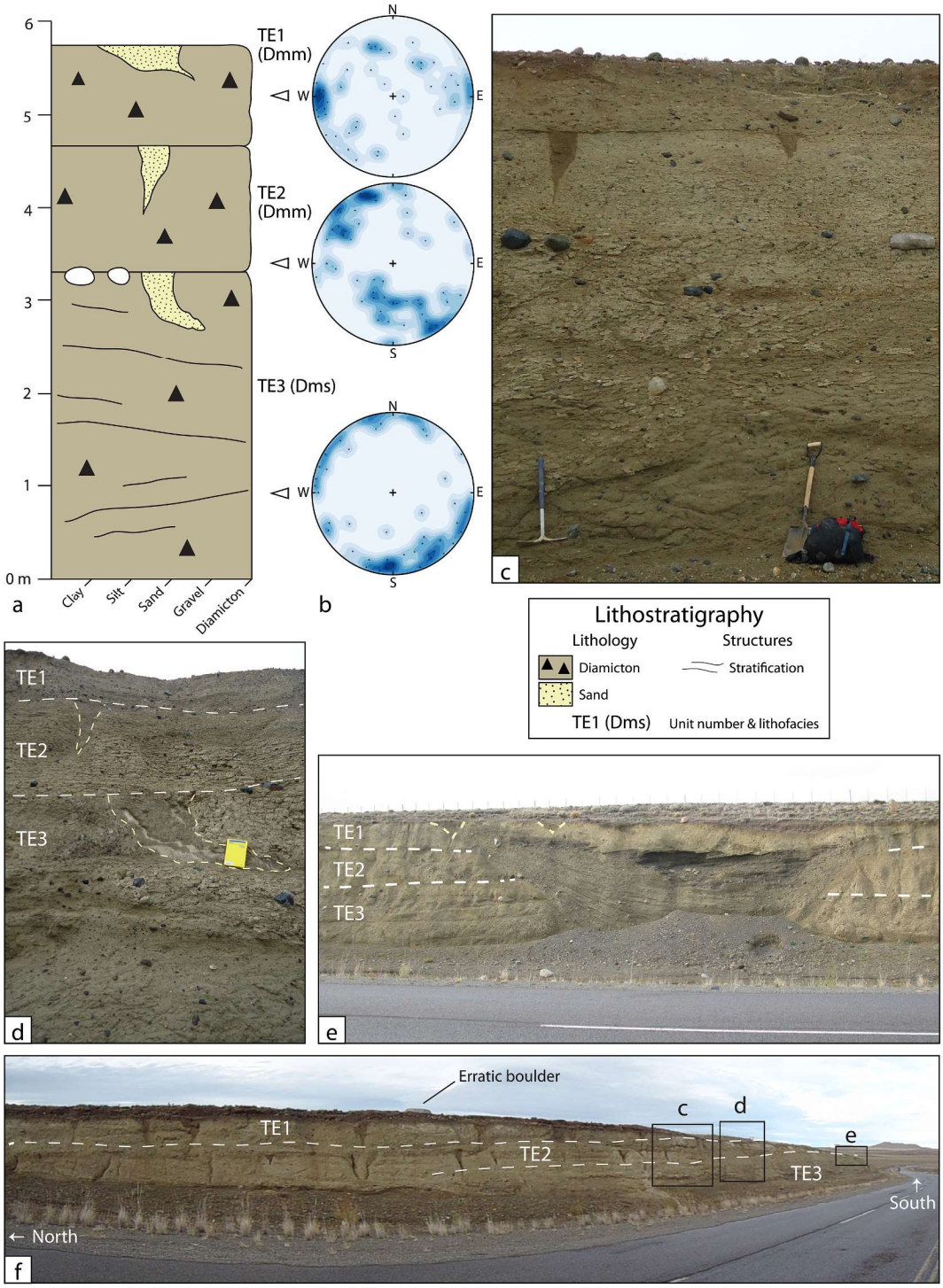

Fig. 10. The Tres de Enero road cut. a) Stratigraphic column. b) Contoured stereonets showing long-axis orientations of rod-shaped stones at the base of units TE1, TE2, and TE3 (lower hemisphere projection). c) Photo of the section on which the drawing in panel a is based. d) Deformed sand wedge extending downward from the contact between units TE2 and TE3. e) Channel fill at the south end of the exposure. f) Photo of the road cut showing lateral continuity of units and locations of photos c, d, and e.

grounding line (Powell, 1990). The ice mass may have been grounded in some places and floating in others at the terminus. Gravel and sand enter standing water at the base of the water column rather than at the top as in the case of a delta. These coarse sediments typically display planar bedding characteristic of the upper flow regime, which is distinct from the typical bedding of fluvial or glaciofluvial deposits. Benn (1996) describes subaqueous moraines composed of gravel and sand with interbeds of diamictic debris flow deposits delivered from the glacier grounding line. A similar environment is envisioned at Cabo Vírgenes, where stratified deformed beds of diamicton are interlayered with gravel and sand beds.

Foreset bedding, indicative of delta deposits, is not present in any of the Cabo Vírgenes sections; thus the sediments were not deposited at the mouths of terrestrial streams. Some of the gravel and diamicton lenses and beds occupy channels, indicating that there was sufficient energy to scour and fill underlying eroded channel floors. A sloping surface can be

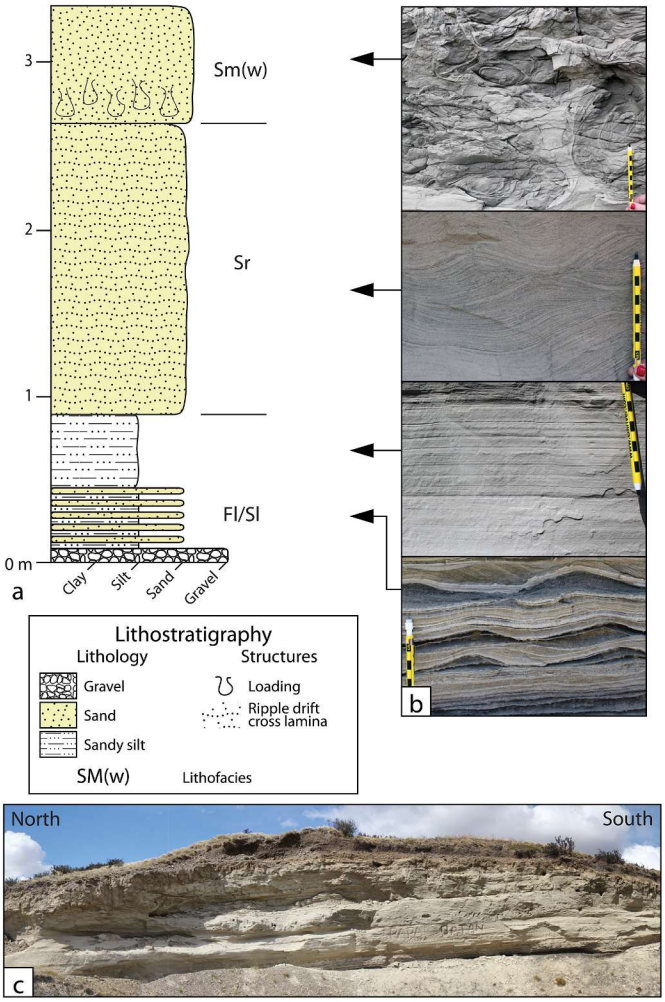

Fig. 11. The Estancia Chimen Aike section. a) Stratigraphic column Sm(w) = massive sand with loaded base; Sr = rippled sand; Fl = laminated sandy silt; Fl = laminated sand. b) Photos showing sedimentary structures within the sequence. c) Photograph of the borrow pit exposure.

inferred from the widespread occurrence of mass flow deposits, which in subaqueous grounding-line fans results from the failure and mobilization of rapidly accumulating sediment. This process produces stratified diamicton units within eroded channels (Bennett et al., 2002). Mass flow deposits also become better sorted and finer-grained with distance from tunnel mouths and other sediment sources due to a decrease in flow velocities. In general, unit CV2 records ice-rafted rain-out debris or deposition by mass flows on the distal margins of fans or perhaps beyond, whereas unit CV1 clearly is a product of ice-proximal deposition near the apexes of the fans.

Deformation structures are common in subaqueous grounding-line sediments (Powell, 1990; Benn, 1996; Bennett et al., 2002). Ball-and-pillow and flame structures are produced by pene-contemporaneous deformation of loose water-saturated sediments as they compact and dewater. The deformation of some diamicton layers suggests sliding or flow of sediment along unstable surfaces. Localized glacier readvance may have produced faults and folds in unit CV2.

The contact between CV2 and CV3, where exposed, is planar, sharp, and erosive. There is no evidence of deformation of CV3, which is so characteristic of units CV1 and CV2; therefore we ascribe CV3 to an older (GPG) glaciation. We interpret the unit to be a till, most likely a subglacial till due to its massive structure, horizontal jointing, faceted and striated clasts, and high density.

A question arises as to whether units CV1 and CV2 were deposited in

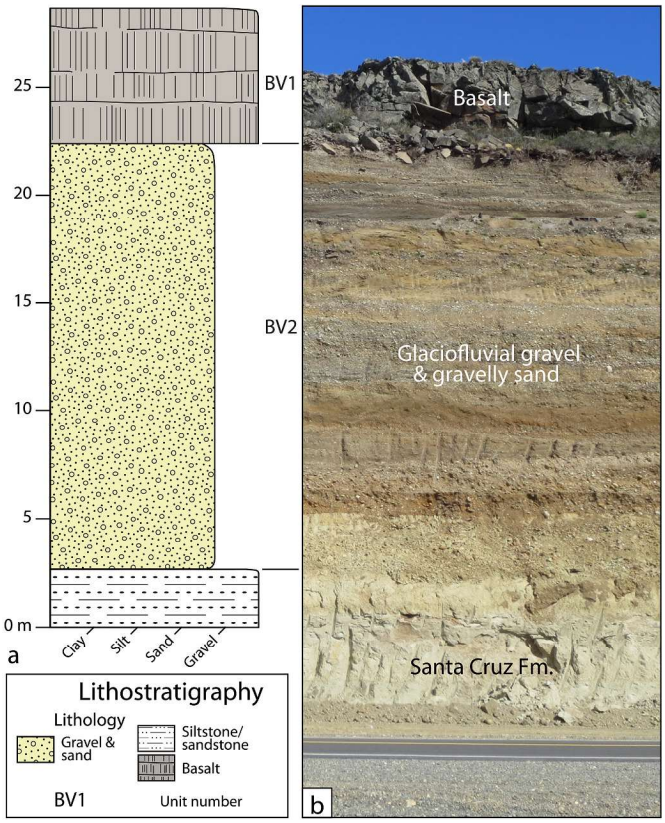

Fig. 12. a) Stratigraphic log and b) photo of the Bella Vista section.

freshwater or a marine environment. Glacio-isostatic depression related to the advance of ice along the Strait of Magellan would be expected to lower the land surface, although not necessarily enough to compensate for the large eustatic drawdown of the sea at the maximum of the Cabo Vírgenes glaciation. Because of uncertainty in the age of this glaciation, the magnitude of eustatic sea-level lowering is unknown. However, it likely was large given the much greater extent of the glaciers during this glaciation than during MIS 2 (Coronato and Rabassa, 2011). Even with an extreme lowering of sea level, however, there is no reasonable configuration of glaciers that would impound an ice-dammed lake in the vicinity of Cabo Vírgenes and that would provide a freshwater environment in which units CV1 and CV2 could accumulate. Yet, there are no marine macrofossils in these units in spite of the excellent exposure. Neither were any marine or freshwater diatoms or foraminifera found in a bulk sample of unit CV2. It thus seems unlikely that these sediments are glaciomarine.

We hypothesize that units CV1 and CV2 were deposited in a standing body of freshwater with accommodation space of up to 70 m at the toe of the ice sheet. We propose that this water body was created by differential glacio-isostatic downwarping of the crust at the periphery of the ice sheet, forming a moat that trapped freshwater from the melting ice front (Clague and Griffing, 2014). The alternative, that glacio-isostatic depression exceeded eustatic sea-level lowering at the peak of the Cabo Vírgenes glaciation, although possible, is not supported by the absence of marine fossils in units CV2 and CV2.

4.2. *Cabo del Espíritu Santo*

The Cabo del Espíritu Santo surface was mapped by Meglioli (1992) as GPG, but later assigned to the Cabo Vírgenes glaciation by Coronato et al. (2004a). The sediment sequence at this site includes two packages of glacial advance sediments, each consisting of outwash overlain by subglacial till. We consider the sand/gravel units (ES3 and ES5) to be

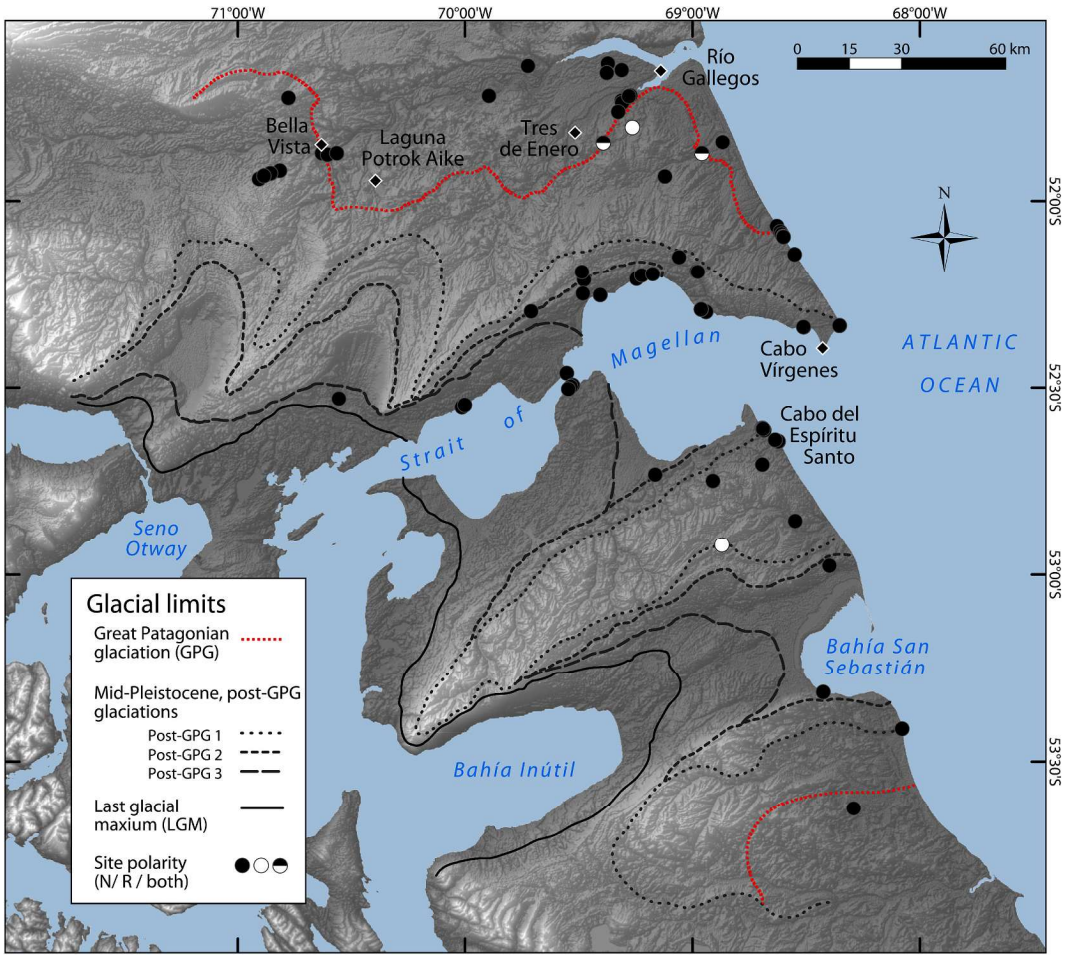

Fig. 13. Magnetic polarity of samples analyzed in this study in relation to maximum glacial limits of Meglioli (1992). See Appendix Table 1 for data.

advance outwash due their cross-bedding, upward coarsening, and poor sorting. The lower glacial package must be GPG in age based on the mapping of Meglioli (1992). The upper package is either GPG if the interpretation of Meglioli (1992) is correct, or Cabo Vírgenes if Coronato et al. (2004a) are correct. A third cold event is recorded by the sand wedges developed in the upper till.

The sediments at Cabo del Espíritu Santo are very different from those at Cabo Vírgenes. There is no evidence of the subaqueous environments in which units CV1 and CV2 were deposited at Cabo Vírgenes. Although the Cabo del Espíritu Santo sequence overlies a bedrock strath, it is topographically higher than much of sequence at Cabo Vírgenes.

There are several possible explanations for the difference in the sediments at the two localities, but we favor differential glacio-isostatic depression of the crust as the most likely explanation. As mentioned above, units CV1 and CV2 were deposited in standing water (very likely freshwater), and therefore a glacio-isostatically depressed moat must have been present at Cabo Vírgenes and the Atlantic continental shelf to the east. We suggest that either such a moat did not exist on northeast Tierra del Fuego where bedrock is exposed above sea level, or that the magnitude of glacio-isostatic depression there was less than at Cabo Vírgenes.

4.3. *Tres de Enero*

The Tres de Enero road cut provides clear evidence for at least three glaciations involving advances of the Magellan ice lobe at least as far east as 69°W during the GPG. Each of the three glaciations was followed by a period during which climate was cold enough for ice-wedges to form on the glacier-free surface. Our interpretation that the three till units were deposited during three glaciations over a long period of time is supported by the change in magnetic polarity from reversed to normal between deposition of units TE3 and TE2 (Fig. 10).

There are several possible interpretations of the sequence of events recorded at this locality. One possibility is that the lowest, reversed till (unit TE3) was deposited late in the late Matuyama Reversed Chron (0.991–0.780 Ma), and the two normal tills (units TE1 and TE2) were deposited during the Brunhes Normal Chron (<0.780 Ma) (Fig. 19). This interpretation requires post-GPG ice lobes to have extended farther east and north than mapped by Meglioli (1992) and Coronato et al. (2004a). It also requires that TE1 and TE2 were deposited during MIS 16 and MIS 18, respectively (Fig. 19). Finally, this first possibility (i.e. both TE1 and TE2 are Brunhes in age) is in accord with, although not required by, an interpretation that the lowest till in the Cabo Virgenes seacliff sections (unit CV3) correlates with unit TE1 or unit TE2.

A second possibility is that the reversely magnetized till was deposited late during the Matuyma Reversed Chron, but before the Jaramillo Normal subchron, and the lower normal till dates to the Jaramillo Subchron (1.075–0.991 Ma; MIS 30). In this case, only the upper normal till (TE1) would date to the Brunhes Normal Chron. Furthermore, in such a scenario and given that the Tres de Enero site is outside the Cabo Virgenes drift limit, unit TE1 would likely correlate with unit CV3 (e.g. MIS18) and would be older than units CV1 and CV2 (e.g., MIS 16).

A third possibility is that both of the normally magnetized tills at Tres de Enero date to the Jaramillo subchron (MIS 30). Although possible, this interpretation seems least likely because it requires that two

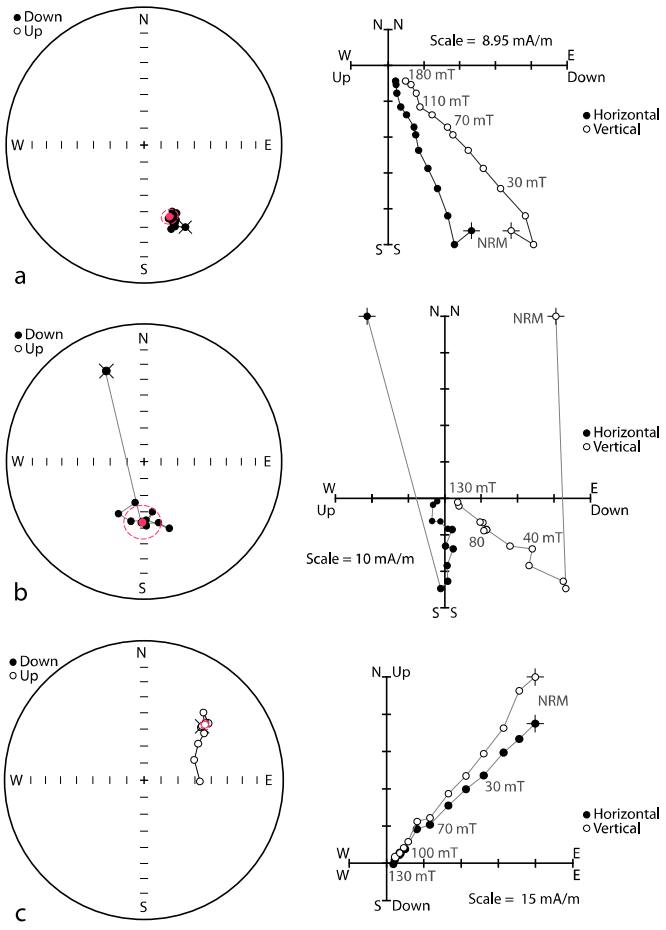

Fig. 14. Stereographic plots (Lambert equal-area) projections (left) and orthogonal plots (right) for a) a reversed polarity sample, b) a reversed polarity sample with a weak normal overprint, and c) a normal polarity sample. Stereographic plots show the change in magnetic directions for each AF cleaning step plotted relative to present horizontal.

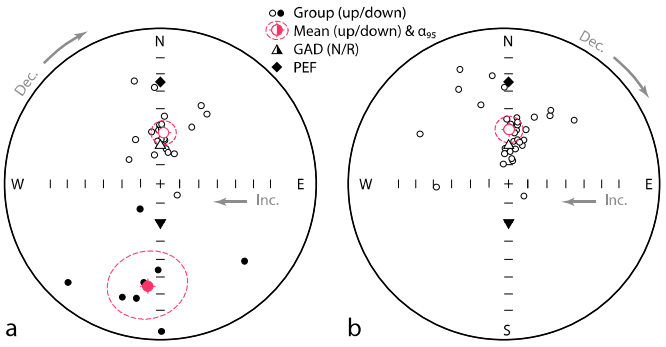

Fig. 15. Stereographic plot of means and 95% circles of confidence (dashed line) for a) GPG drift and b) Cabo Vírgenes drift, which post-dates the GPG. The mean direction of each drift unit is in close agreement with the geocentric axial dipole (GAD; inclination = −68.6°). Individual data points are units within each of the drift sheets and are listed in Appendix Table 1.

glaciations separated by a non-glacial interval during which sand wedges formed occurred within the 84 ka span of the Jaramillo subchron. Further, the astronomically tuned, benthic oxygen isotope record (Lisiecki and Raymo, 2015) indicates that there was only one cold period (MIS 30) during this subchron.

Whichever interpretation is correct, glaciers extended to and probably beyond the modern Atlantic coastline two or three times in Early and Middle Pleistocene (Cabo Vírgenes units CV1/2 and CV3; and Tres de Enero units TE1, TE2, and TE3). At least one of the Tres de Enero advances (recorded by unit TE3) is older than the Cabo Vírgenes glaciation.

Table 1
Means of magnetic data for sample groups by glaciation and polarity.

Group	*D*	*I*	N	*k*	α_{95}
GPG (all samples)	25.8	−73.5	29	2.0	7.6
GPG (N-polarity samples)	3.6	−63.0	20	24.5	6.4
GPG (R-polarity samples)	166.6	41.6	9	8.0	19.4
Cabo Vírgenes (all samples)	0.2	−60.5	31	7.7	9.6

4.3.1. *Estancia Chimen Aike*

The glaciolacustrine sediments at Estancia Chimen Aike are magnetically reversed and thus older than 0.780 Ma. We have no further chronological control on the age of these sediments, but note that they are near the inferred outer limit of GPG glaciation in the Río Gallegos area. They may correlate with unit TE3 at the Tres de Enero locality, which is also magnetically reversed.

4.3.2. *Bella Vista*

Samples for paleomagnetic analysis from three lenses of sandy silt within the outwash gravel 1 m and 14 m above its lower contact with the Santa Cruz Formation have normal polarity. A third set of samples 18 m above the base of the unit has transitional polarity. We assign this gravel to the GPG, as it is normally magnetized but older than 0.89 Ma, the age of the overlying basalt flow; it may have been deposited during the Jaramillo subchron. The transitional polarity of the sample in the upper part of the unit may indicate that the gravel was deposited close to the change from normal to reversed polarity at the end of the Jaramillo subchron (cf. Singer et al., 2004b). We hypothesize that the glaciofluvial gravels indicate that ice was nearby in the Río Gallegos valley during the Jaramillo subchron, most likely during MIS 30. We also suggest that these glaciofluvial gravels might have been deposited at the same time as one of the normally magnetized tills at the Tres de Enero locality. Coronato et al. (2013) describe GPG till deposited by the Magellan glacier lobe near Laguna Potrok Aike that overlies a basalt flow dated 1.19 ± 0.02 Ma (Zolitschka et al., 2006), as well as an outwash fan overlain by a 0.89 ± 0.03 Ma flow (Corbella et al., 2014). The Bella Vista road cut stratigraphy indicates that ice was also present at this time in the Río Gallegos valley.

5. Conclusions

The most extensive ice sheets in southern Patagonia formed in the Early and Middle Pleistocene. They extended east beyond the modern Atlantic shoreline and the mouth of the Strait of Magellan. Thick glacial and proglacial sediments were deposited during the Great Patagonian Glaciation (GPG) and the less-extensive Cabo Vírgenes glaciation.

We report stratigraphic, sedimentologic, and paleomagnetic evidence for at least three Pleistocene glaciations in seacliffs along the Atlantic coast of southern Patagonia and Tierra del Fuego and in road cuts to the west. Up to 70 m of drift consisting of till and planar-bedded gravel and sand with large-scale deformation structures is exposed in a 36-km-long coastal bluff transect north of the Cabo Vírgenes lighthouse at the mouth of the Strait of Magellan. Lithologies and facies associations, unit contacts, and penecontemporaneous deformation of strata indicate deposition in the standing water of what we interpret to be a glacio-isostatically formed, freshwater moat in a grounding-line environment. The sediments are normally magnetized and have no signs of magnetic overprinting and therefore are provisionally assigned to the Brunhes Chron, which spans the past 0.780 Ma. The base of the Cabo Vírgenes drift is exposed in seacliff at the north end of the transect.

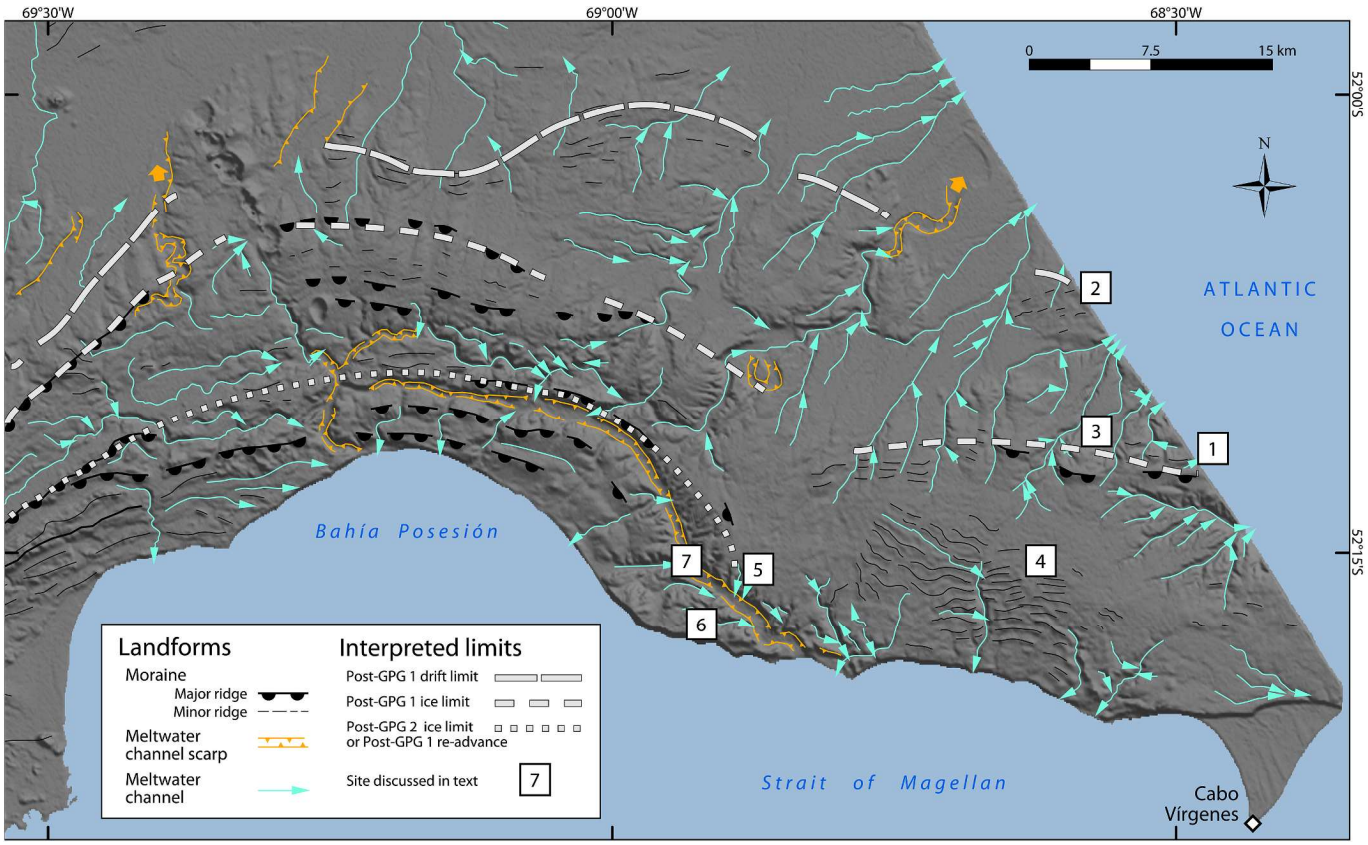

Fig. 16. Interpreted post-GPG 1 (Cabo Vírgenes) sediments and landforms (see text for details of sites 1–7).

Fig. 17. Folded and faulted, glaciolacustrine silt and sand exposed near site no. 4 in Fig. 16), north of the Strait of Magellan. The exposure is about 4.5 m high.

There, it overlies up to 2 m of massive dense subglacial till, likely deposited during a Great Patagonian glaciation.

Two tills and associated outwash are exposed in the Cabo del Espíritu Santo seacliff on Tierra del Fuego at the Argentina-Chile border. This sequence records two advances of glaciers that reached the Atlantic coast during the Early and Middle Pleistocene. The Cabo del Espíritu Santo seacliff sections are situated on the south side of the Strait of Magellan ice lobe at the same distance from the Andes as the Cabo Virgenes seacliff sections, which are located on the north side of the Strait. This correspondence suggests that the Cabo del del Espíritu Santo

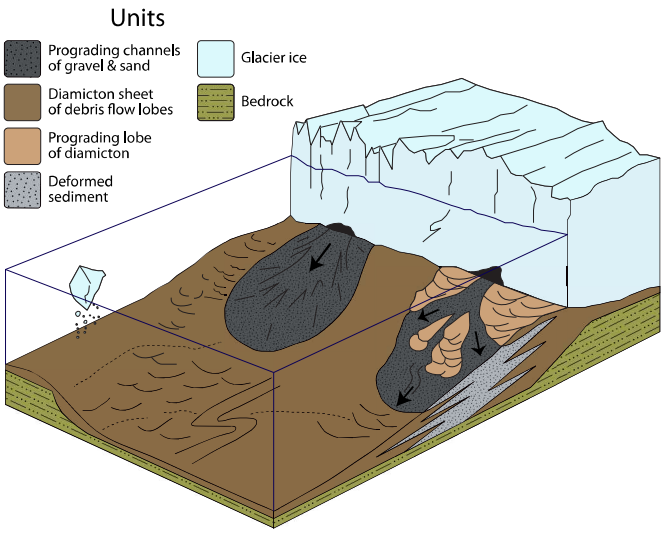

Fig. 18. Schematic diagram showing a glacial grounding-line environment (modified from Bennett et al., 2002).

sequence tills may record the same advances as units in the Cabo Vírgenes seacfliff (units CV1/CV2 and CV3). The depositional environments, however, are different – there is no evidence for the grounding-line glaciolacustrine environment represented by units CV1 and CV2 at Cabo del Espíritu Santo.

A highway cut (Tres de Enero) about 90 km northwest of Cabo Vírgenes exposes three subglacial tills – two normally magnetized tills, at least one of which, and perhaps, both date to the early Brunhes Chron, and a lower reversely magnetized till, probably deposited late during the preceding Matuyama Chron. Sand wedges extend down from the top of each till, indicating that permafrost formed at the ground surface after each of the three tills was deposited and, therefore, that the tills record three separate glaciations. The reversely magnetized till and other reversely magnetized sediments within the limits of the GPG indicate that the earliest and most extensive Pleistocene glaciations occurred before 0.780 Ma. They further show that the GPG is not a single glaciation, but rather a composite of at least three, and perhaps many more, glaciations. In the Río Gallegos Valley, a 0.89 Ma basalt flow caps a thick unit of normally magnetized glaciofluvial gravel, which may have been deposited late during the Jaramillo subchron (just before 0.991 Ma).

Declaration of competing interest

The authors declare that they have no known competing financial interests or personal relationships that could have appeared to influence

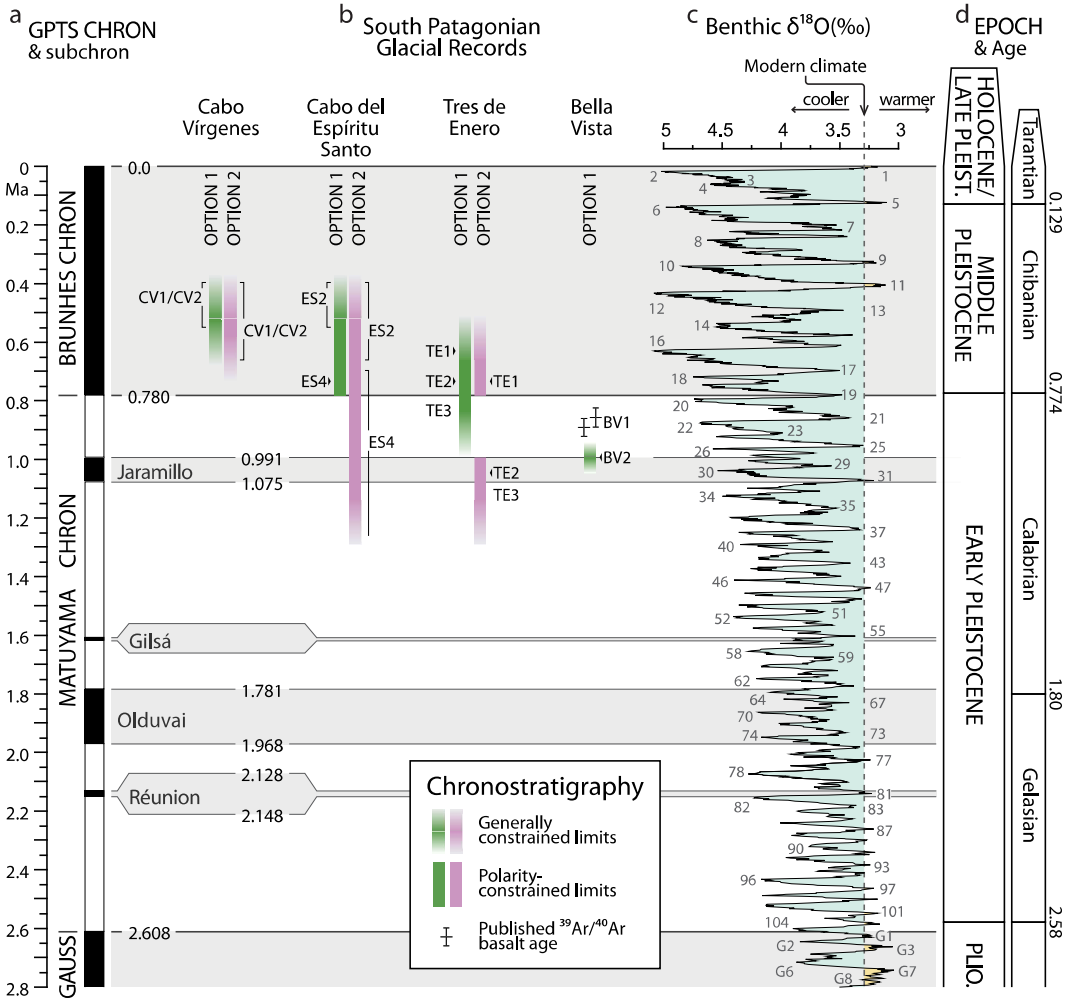

Fig. 19. Timing of Early and Middle Pleistocene glaciation of southern Patagonian. a) LR04 Geomagnetic Polarity Time Scale (GPTS) with two short-lived normal polarity periods based on Channell et al. (2002) (Gilsa event) and (Ogg, 2012) (Reunion subchron). b) Age constraints of glacial records described in the text. c) LR04 benthic $\delta^{18}O$ paleo-temperature profile derived from 57 globally distributed records with odd and even Marine Isotope Stages (MIS), indicating, respectively, glacial and interglacials. d) Geologic Time Scale. LR04 record is from Lisiecki and Raymo (2005), and the Geologic Time Scale is from Gibbard and Head (2021).

the work reported in this paper.

Acknowledgements

This research was supported by the Natural Sciences and Engineering Research Council (NSERC) through Discovery Grants to Barendregt and Clague (grant numbers 0581 and 24595), and Canada Research Chair (CRC) funds to Clague. We thank journal reviewer Philip Gibbard for his thoughtful and helpful comments on a draft of the paper.

Appendix A. Supplementary data

Supplementary data to this article can be found online at https://doi.org/10.1016/j.jsames.2021.103687.

References

Benn, D.I., 1996. Subglacial and subaqueous processes near a glacier grounding line: sedimentological evidence from a former ice-dammed lake, Achnasheen, Scotland. Boreas 25 (1), 23–36.
Benn, D.I., Evans, D.J., 2010. Glaciers & Glaciation, second ed. Hodder Education, London.
Bennett, M.R., Huddart, D., Thomas, G.S.P., 2002. Facies architecture within a regional glaciolacustrine basin: copper River, Alaska. Quat. Sci. Rev. 21 (20), 2237–2279.
Bockheim, J., Coronato, A., Rabassa, J., Ercolano, B., Ponce, J., 2009. Relict sand wedges in southern Patagonia and their stratigraphic and paleo-environmental significance. Quat. Sci. Rev. 28 (13–14), 1188–1199.
Boulton, G.S., 1986. Push moraines and glacier-contact fans in marine and terrestrial environments. Sedimentology 33 (5), 677–698.
Butler, R.F., 1992. Paleomagnetism; Magnetic Domains to Geologic Terranes. Blackwell Scientific Publishers, Boston, MA.
Caldenius, C.R.C., 1932. Las glaciaciones cuaternarias en la Patagonia y Tierra del Fuego: una investigación regional, estratigráfica y geocronológica, una comparación con la escala geocronológica sueca. Geogr. Ann. 14 (1–2), 1–164.
Chadima, M., Hrouda, F., 2006. Remasoft 3.0 – a user-friendly paleomagnetic data browser and analyzer. Travaux Géophysiques 27, 20–21.
Channell, J.E.T., Mazaud, A., Sullivan, P., Turner, S., Raymo, M.E., 2002. Geomagnetic excursions and paleointensities in the Matuyama chron at ocean drilling program sites 983 and 984 (Iceland basin). J. Geophys. Res. 107 (B6) https://doi.org/10.1029/2001JB000491. EPM 1-EPM 1-14.1.
Clague, J.J., Griffing, C.Y., 2014. Deposition in glacio-isostatic moats in coastal environments. Geological Society of America, Abstracts with Programs 46 (6), 265.
Clague, J.J., Barendregt, R.W., Menounos, B., Roberts, N.J., Rabassa, J., Martinez, O., Ercolano, B., Corbella, H., 2020. Pliocene and early Pleistocene glaciation and landscape evolution on the patagonian steppe, Santa Cruz province, Argentina. Quat. Sci. Rev. 227, 105992.
Corbella, H., 2002. El campo volcano-tectónico de Pali Aike. In: Haller, M.J. (Ed.), Geologia y Recursos Naturales de Santa Cruz. Asociación Geológica Argentina, pp. 285–301.
Corbella, H., Ercolano, B., Tiberi, P., Coronato, A., Malderwald, B., 2014. Basaltos del valle Gallegos Chico, naturaleza, edad y significado, provincia de Santa Cruz, Patagonia Austral. XIX Congreso Geologico Argentino, Actas S13-12, Cordoba, pp. 2–5. Junio.
Coronato, A., Rabassa, J., 2011. Pleistocene glaciations in southern Patagonia and Tierra del Fuego. In: Ehlers, J., Gibbard, P.L., Hughes, P.D. (Eds.), Quaternary Glaciations: Extent and Chronology: A Closer Look, Developments in Quaternary Science, vol. 15. Elsevier, Amsterdam, pp. 715–727.
Coronato, A., Ercolano, B., Corbella, H., Tiberi, P., 2013. Glacial, fluvial and volcanic landscape evolution in the Laguna Potrok Aike maar area, Southern Patagonia, Argentina. Quat. Sci. Rev. 71, 13–26.
Coronato, A., Martínez, O., Rabassa, J., 2004a. Glaciations in Argentine Patagonia, southern South America. In: Ehlers, J., Gibbard, P.L. (Eds.), Quaternary Glaciations: Extent and Chronology, Part III: South America, Asia, Africa, Australasia, Antarctica, Developments in Quaternary Science, vol. 2. Elsevier, Amsterdam, pp. 49–67.
Coronato, A., Meglioli, A., Rabassa, J., 2004b. Glaciations in the Magellan Straits and Tierra del Fuego, southernmost South America. In: Ehlers, J., Gibbard, P.L. (Eds.), Quaternary Glaciations: Extent and Chronology, Part III: South America, Asia, Africa, Australasia, Antarctica, Developments in Quaternary Science, vol. 2. Elsevier, Amsterdam, pp. 45–48.
Deblonde, C., Plouffe, A., Boisvert, E., Buller, G., Davenport, P., Everett, D., Inglis, E., Kerr, D., Moore, A., Paradis, S.J., 2012. Science Language for an Integrated Geological Survey of Canada Data Model for Surficial Maps. Version 1.2. Geological Survey of Canada, Open File, p. 7003.
D'Orazio, M., Agostini, S., Mazzarini, Fl, Innocenti, F., Manetti, P., Haller, M., Lahsen, A., 2000. The Pali Aike volcanic field, Patagonia: slab-window magmatism near the tip of south America. Tectonophysics 321 (4), 407–427.
Evans, D.J.A., Benn, D.I., 2004. A Practical Guide to the Study of Glacial Sediments. Routledge, New York.
Eyles, N., Eyles, C.H., Miall, A.D., 1983. Lithofacies types and vertical profile models; an alternative approach to the description and environmental interpretation of glacial diamict and diamictite sequences. Sedimentology 30 (3), 393–410.
Gibbard, P.L., Head, M.J., 2020. Chapter 30 – the quaternary period. In: Gradstein, F.M., Ogg, J.G., Schmitz, M.D., Ogg, G.M. (Eds.), Geological Timescale 2020, vol. 2. Elsevier, pp. 1217–1255. https://doi.org/10.1016/B978-0-12-824360-2.00030-9.
Gorring, M.L., Kay, S.M., Zeitler, P.K., RamosM, V.A., Rubiolo, D., Fernandez, M.I., Panza, J.L., 1997. Neogene Patagonian plateau lavas: continental magmas associated with ridge collision at the Chile Triple Junction. Tectonics 16 (1), 1–17.
Griffing, C.Y., 2018. Late Cenozoic Glaciations and Environments in Southernmost Patagonia. PhD Thesis. Simon Fraser University, Burnaby, BC.
Griffing, C.Y., Clague, J.J., Barendregt, R.W., Menounos, B., Hemming, S.R., Rabassa, J., Ercolano, B., Martinez, O., 2020. Pliocene-Pleistocene landscape evolution and watershed reorganization east of the central Andes in Argentine Patagonia. In: Waitt, R.B., Thackray, G.D., Gillespie, A.R. (Eds.), Untangling the Quaternary Period: A Legacy of Stephen C. Porter, vol. 548. Geological Society of America Special Paper. https://doi.org/10.1130/2020.2548(02.
Kirschvink, J.L., 1980. The least-squares line and lane and the analysis of palaeomagnetic data. Geophys. J. Roy. Astron. Soc. 62 (3), 699–718.
Lagabrielle, Y., Calabrino, B., Suárez, M., Ritz, J.-F., 2010. Mio-Pliocene glaciations of Central Patagonia: new evidence and tectonic implications. Andean Geol. 37 (2), 276–299.
Lisiecki, L.E., Raymo, M.E., 2005. A Pliocene-Pleistocene stack of 57 globally distributed benthic δ18O. Paleoceanography 20, PA1003.
Mazzarini, F., D'Orazio, M., 2003. Spatial distribution of cones and satellite-detected lineaments in the Pali Aike Volcanic Field (southernmost Patagonia): insights into the tectonic setting of a Neogene rift system. J. Volcanol. Geoth. Res. 125 (3), 291–305.
Meglioli, A., 1992. Glacial Geology and Chronology of Southernmost Patagonia and Tierra del Fuego, Argentina and Chile. PhD thesis. Lehigh University, Bethlehem, PA.
Mejia, V., Opdyke, N.D., Vilas, J.F., Singer, B.S., Stoner, J.S., 2004. Plio-Pleistocene time-averaged field in southern Patagonia recorded in lava flows. G-cubed 5 (3), 1–15.
Mercer, J.H., 1976. Glacial history of southernmost South America. Quat. Res. 6 (2), 125–166.
Mercer, J.H., 1983. Cenozoic glaciation in the southern hemisphere. Annu. Rev. Earth Planet Sci. 11 (1), 99–132.
Mercer, J.H., Sutter, J.F., 1982. Late Miocene—earliest Pliocene glaciation in southern Argentina: implications for global ice-sheet history. Palaeogeogr. Palaeoclimatol. Palaeoecol. 38 (3), 185–206.
Mercer, J.H., Fleck, R.J., Mankinen, E.A., Sander, W., 1973. Southern Patagonia; glacial events between 4 m.y. and 1 m.y. ago. In: Suggate, R.P., Cresswell, M.M. (Eds.), Quaternary Studies. Royal Society New Zealand, Wellington, pp. 223–230.
Ogg, J.G., 2012. Geomagnetic polarity time scale. Chapter 5. In: Gradstein, F., Ogg, J.G., Schmitz, M., Ogg, G. (Eds.), The Geologic Time Scale 2012. Elsevier, Amsterdam, pp. 85–113.
Perkins, M.E., Fleagle, J.G., Heizler, M.T., Nash, B., Bown, T.M., Tauber, A.A., Dozo, M. T., 2012. Tephrochronology of the Miocene Santa Cruz and pinturas formations, Argentina. In: Vizcaíno, S.F., Kay, R.F., Bargo, M.S. (Eds.), Early Miocene Paleobiology in Patagonia: High-Latitude Paleocommunities of the Santa Cruz Formation. Cambridge University Press, Cambridge, pp. 23–40.
Powell, R.D., 1990. Glacimarine processes at grounding-line fans and their growth to ice-contact deltas. In: Dowdeswell, J.A., Scourse, J.D. (Eds.), Glaciomarine Environments: Processes and Sediments, vol. 53. Geological Society of London Special Publications, pp. 53–73.
Powell, R.D., Alley, R.B., 1997. Grounding-line systems: processes, glaciological inferences and the stratigraphic record. In: Barker, P.F., Cooper, A.K. (Eds.), Geology and Seismic Stratigraphy of the Antarctic Margin, 2, vol. 71. Antarctic Research Series, pp. 169–187.
Powell, R.D., Cooper, J.M., 2014. A glacial sequence stratigraphic model for temperate, glaciated continental shelves. In: Dowdeswell, J.A., Cofaigh, O. (Eds.), Glacier-influenced Sedimentation on High-Latitude Continental Margins, vol. 203. Geological Society of London Special Publications, pp. 215–244.
Rabassa, J., 2008. Late Cenozoic glaciations in Patagonia and Tierra del Fuego. In: Rabassa, J. (Ed.), The Late Cenozoic of Patagonia and Tierra del Fuego, Developments in Quaternary Science, vol. 11. Elsevier, Amsterdam, pp. 151–204.
Rabassa, J., Clapperton, C.M., 1990. Quaternary glaciations of the southern Andes. Quat. Sci. Rev. 9 (2–3), 153–174.
Rabassa, J., Coronato, A., 2009. Glaciations in Patagonia and Tierra del Fuego during the Ensenadan Stage/Age (Early Pleistocene-earliest Middle Pleistocene). Quat. Int. 210 (1–2), 18–36.
Rabassa, J., Coronato, A., Martinez, O., 2011. Late Cenozoic glaciations in Patagonia and Tierra del Fuego: an updated review. Biol. J. Linn. Soc. 103 (2), 316–335.
Ramos, V.A., 1989. Andean foothills structures in northern Magallanes Basin, Argentina. AAPG (Am. Assoc. Pet. Geol.) Bull. 73, 887–903.
Singer, B.S., Ackert Jr., R.P., Guillou, H., 2004a. $^{40}Ar/^{39}Ar$ and K-Ar chronology of Pleistocene glaciations in Patagonia. Geol. Soc. Am. Bull. 116 (3–4), 434–450.
Singer, B.S., Brown, L.L., Rabassa, J.O., Guillou, H., 2004b. 40Ar/39Ar chronology of late Pliocene and early Pleistocene geomagnetic and glacial events in southern Argentina. In: Channell, J.E.T., Kent, D.V., Lowrie, W., Meert, J.G. (Eds.), Timescales of the Internal Geomagnetic Field. American Geophysical Union, Washington, D.C., pp. 175–190
Ton-That, T., Singer, B., Mörner, N.-A., Rabassa, J., 1999. Datación de lavas basálticas por 40Ar/39Ar y geología glacial de la región del lago Buenos Aires, Provincia de Santa Cruz, Argentina. Rev. Asoc. Geol. Argent. 54 (4), 333–352.
Wenzens, G., 2000. Pliocene piedmont glaciation in the Río shehuen valley, southeast Patagonia, Argentina. Arctic Antarct. Alpine Res. 32 (1), 46–54.

Wenzens, G., 2006. Terminal moraines, outwash plains, and lake terraces in the vicinity of Lago Cardiel (49°S; Patagonia, Argentina) – evidence for Miocene Andean foreland glaciations. Arctic Antarct. Alpine Res. 38 (2), 276–291.

Zambrano, Y., Urien, C.M., 1970. Geological outline of the basin in Southern Argentina and their continuation off the Atlantic shore. J. Geophys. Res. 75 (8), 1363–1396.

Zolitschka, B., Schäbitz, F., Lücke, A., Corbella, H., Ercolano, B., Fey, M., Haberzettl, T., Janssen, S., Maidana, N., Mayr, C., Ohlendorf, C., Oliva, G., Paez, M.M., Schleser, G. H., Soto, J., Tiberi, P., Wille, M., 2006. Crater lakes of the Pali Aike Volcanic Field as key sites for paleoclimatic and paleoecological reconstructions in southern Patagonia, Argentina. J. S. Am. Earth Sci. 21 (3), 234-3.